THERMAL CONDUCTIVITY OF DIAMOND THIN-FILMS ON SILICON WAFERS

By

MARSHALL HARRUP

Bachelor of Science in Engineering Physics

Oral Roberts University

Tulsa, Oklahoma

2013

Submitted to the Faculty of the
Graduate College of the
Oklahoma State University
in partial fulfillment of
the requirements for
the Degree of
MASTER OF SCIENCE
December, 2015

THERMAL CONDUCTIVITY OF DIAMOND THIN-FILMS ON SILICON WAFERS

Thesis Approved:

Dr. Raj Singh

Thesis Adviser

Dr. Ranji Vaidyanathan

Dr. Pankaj Sarin

ACKNOWLEDGEMENTS

I would like to thank my advisor, Dr. Raj Singh, for allowing me to work on this project and accepting me into his research group. The knowledge and skills I have gained over the course of this research will be instrumental to my future endeavors. I would also like to thank my Principal Investigator, Dr. Nirmal Govindaraju, for his guidance and assistance through all the iterations of this research. I appreciate the guidance of Dr. Ranji Vaidyanathan and Dr. Pankaj Sarin, and for their service on my thesis committee.

To my parents, Blake and Corinne, thank you for ensuring I was on the path God had for me, and for teaching me to dream big. To my siblings, thank you for giving me a reason to be an example and for always cheering me on. To my extended family, thank you for encouraging me so much over the years.

And finally, to Amanda, thank you for being the most loving and constant companion I could have hoped for. You are my best friend, the one I long to see whenever we are separated, and since entering my life you have been the greatest support imaginable. I love you deeply, and am amazingly blessed to spend the rest of my life with you.

Name: MARSHALL HARRUP

Date of Degree: DECEMBER, 2015

Title of Study: THERMAL CONDUCTIVITY OF DIAMOND THIN-FILMS ON SILICON WAFERS.

Major Field: MATERIALS SCIENCE AND ENGINEERING

Synthetic diamond films may play an important role in thermal management of processors. Diamond may be up to four times as thermally conductive as copper, but the conductivity of individual films may vary based on synthesis parameters. Therefore a straightforward nondestructive method is desired to determine thermal characteristics of diamond-coated silicon wafers. Diamond-coated samples were grown via Microwave-Plasma Chemical Vapor Deposition, and characterized for film thickness by pre- and post-deposition weighing and film quality by Raman spectroscopy. The thermal conductivity of samples is measured by three different methods: thermocouples, infrared camera, and Raman spectroscopy. Each measurement setup is based on Fourier's first law of heat conduction, in which the temperature gradient across a region of material is proportional to the thermal conductivity of the material. Thermocouples were used initially, which allowed for quick feedback on temperature gradients. However, the measurement accuracy was greatly affected by the thermocouple mounting, thus non-contact methods of measurement were considered. Infrared cameras were used to view the temperature profile of the entire system, but it was determined that the surface temperatures visible to the camera were different than the internal temperatures of the experimental setup. Finally, Raman spectroscopy is used to measure temperature and thermal gradient, due to the temperature dependence of the Raman peaks. It was found that the diamond peak of four different films exhibited a thermal shift comparable to published data. This method will be pursued in future research to measure thermal properties of diamond films, including the interfacial thermal characteristics.

TABLE OF CONTENTS

LIST OF TABLES

Table Page

LIST OF FIGURES

CHAPTER I

INTRODUCTION

1.1 Motivation

As electronic devices continue to shrink, adequate thermal management becomes more critical. Smaller devices are more susceptible to damage from overheating, and more challenging to draw heat from due to smaller surface area. Overheating reduces efficiency of systems and increases operating costs. It also degrades components, necessitating replacement. Both labor and downtime costs for repair can be substantial. Effective thermal management allows mechanical and electrical components to last longer and be used more efficiently. This research compares several methods to measure the thermal conductivity of diamond-coated silicon samples. Accurate temperature measurements are important to find the temperature gradients of different films, to create the most effective heat-transfer interfaces for electronic systems. The thermal gradient across a diamond film is a function of that film's conductivity. To find the thermal conductivity of several films, a temperature gradient is established across a film and accurately measured. The thermal properties of the film may be calculated from this temperature drop. Other research groups have used methods that use thermocouples, thin metal films on the diamond's surface, or lasers to measure the thermal properties of diamond thin-films. This research will compare three methods and make a recommendation for future research. This research is unique in that it will focus on using common and low-cost items for measurement, with the goal of finding an approach that low-budget laboratories may use.

Barriers to heat conduction are typically physical; grain boundaries limit the transfer of thermal energy within a material's bulk, and interfaces retard heat transfer between different materials or different devices. Just like light at opaque surfaces, some energy is transmitted and some reflected. When two rough surfaces are in contact, microscopic air pockets form which lessen heat transfer. Convection through air pockets is orders of magnitude less efficient than conduction. Thermal grease may be used to eliminate air gaps; although it is thermally resistive, it allows for more even heat spreading between components. The goal is to find a material that can act as an interface but is itself a good conductor of heat. A potential material is diamond. The properties of this material are well-known and highly attractive to scientists and engineers.

For thermal management, a characteristic of great value is high thermal conductivity. Diamond exhibits this better than nearly any material [1]. Additionally, low electrical conductivity makes it especially suited for heat sinks on processors or other electronic components, without the need for a separate electrically insulating layer [2]. Synthetic diamond can be grown under a wide variety of conditions, with multiple methods and ratios of ingredients [3]. Given the expense and difficulty of growing diamond, it is important to know the most cost-effective way to grow diamond for thermal applications. Not only the bulk material properties must be considered but also the interface properties, as there is a significant temperature drop between diamond and other materials.

1.2 Objective

This research intends to measure the thermal resistance of diamond films grown on silicon wafers under varying conditions, and parse out the contribution of the growth interface to the overall thermal resistance. For systems in which diamond is deposited on a material with disparate lattice characteristics, the thermal resistance of the interface can dominate the overall thermal resistance of the system [4]. By applying Fourier's First Law of Heat Conduction to a physical scenario, it is possible to examine each component of a system in terms of its contribution to the overall thermal resistance. This approach was chosen due to its simplicity and the lack of complicated mathematics, and because it is a steady-state

instead of time-dependent equation. This meant measurement equipment didn't have to be extremely quick to record the thermal properties of the system.

1.3 Approach

For this research, diamond-coated samples were subjected to analysis with multiple methods that allowed establishment and measurement of the temperature gradient across the sample. Measurement techniques were continually refined to gather more reliable and accurate data.

The first method used thermocouples for measurement, as they are simple to setup and use. The second method used infrared cameras to record data over the system as a whole instead of at discrete points. The third method used a Raman Spectrometer for greater accuracy in temperature measurements. The specifics of each method and their results will be discussed in later chapters.

CHAPTER II

REVIEW OF LITERATURE

2.1 Properties of Diamond

For much of history, diamond use has been confined primarily to jewelry. Over time as the material's noteworthy physical properties were discovered, it became sought by scientists as well as royalty. Diamond has been termed a superlative material, with attributes far apart from other materials. Table 1 shows some of these properties.

Table 1 Diamond Properties [1, 4]

Property	Value
Thermal conductivity at 20C	$2*10^{3}$ W/m K
Bulk modulus	$1.2*10^{12}$ N/m2
Compressibility	$8.3*10^{-13}$ m^2/N
Hardness	90 GPa
Optical transparency	Ultraviolet (100nm) to Infrared (100μm)
Speed of sound through diamond	17.5 km/s
Electrical resistivity at room temperature	10^{13} Ω cm
Resists corrosive agents	
Radiation-tolerant	
Is bio-compatible	

In 1797, the single element that makes up diamond was determined: abundant carbon [4]. For over a century, scientists unsuccessfully attempted to create diamond with catalysts. It was not until the 20th century that progress was made, as the thermodynamics and kinetics of diamond were understood better.

Once the first repeatable diamond synthesis was discovered in the 1950s, different methods followed quickly, with each continually refined and used for specific applications [5]. The next several decades saw leaps and bounds in creating this useful, sought-after material, as growth rates were increased from 1 micron per hour to 10.

2.2 Processing of Diamond

Diamond synthesis has progressed through many iterations. Once it was known that diamond consisted of pure carbon, the quest to create favorable conditions for diamond formation began. Of all carbon allotropes, diamond is the most dense [6], and thus high-pressure methods were pursued. High pressure alone was ineffective, but heating the sample under pressure allowed the activation barrier between sp^2 and sp^3 phases to be crossed [1]. The sp^2 phase refers to the hybrid atomic bond arrangement seen in graphite, where three of the four carbon bonds are "in plane" while the fourth, weaker bond is between planes, allowing those planes to slide along each other and separate easily. At room temperature and pressure, this is the thermodynamically stable allotrope; however, the sp^3 bonding arrangement (four bonds in a tetrahedral arrangement) is kinetically stable once it has been formed. In 1963, highly energetic methods were used to create favorable conditions. Detonation synthesis used carbon-based explosive blends to create nanometer-scale diamond particles [7]. Upon ignition, the pressure and heat cause the carbon present to agglomerate in an sp^3 structure. A slower, more controlled method used a hydraulic press and furnace to achieve the pressure and temperature necessary. Diamond seeds were placed in a chamber with a carbon source, and the chamber exposed to pressure between two anvils. The chamber is heated in addition, and the entire process became known as High Pressure High Temperature or HPHT synthesis. The results of this method were typically for industrial use, as small diamond particles from mining operations or detonation synthesis could be converted to diamond grit or low-purity larger stones, and used for cutting and grinding instruments. The HPHT method is still widely used for these purposes today. However, scientists sought ways to take advantage of diamond's other properties; thermal conductivity, optical transparency, and friction and wear resistance. Different methods of

synthesis were sought more suited to such applications; specifically, methods to grow diamond coatings or films. In the 1960s, it was shown that a radically different method could grow diamond via a chemical reaction, and the physical form would be a film rather than a stone [5]. The thermodynamically challenging method of converting graphite to diamond based on the carbon phase diagram could be bypassed. Thus, the focus of diamond synthesis moved from High-Pressure, High-Temperature methods to Chemical Vapor Deposition.

Attempting growth of diamond based on thermodynamic principles requires extreme conditions; carbon's most stable allotrope at room temperature and pressure is graphite, and a substantial activation energy gap of 728 kJ/mol must be crossed to convert it to diamond [6]. However, it was discovered that diamond could be grown chemically from carbon atoms in an activated gas phase. The primary requirement would simply be a template or pattern for carbon to attach to, as well as a method to remove any non-diamond growth.

Individual carbon atoms attached to a tetrahedral bond template resulted in diamond, but this process was slow. Large enough quantities of carbon needed to be in an activated state, and any non-diamond carbon quickly removed, to achieve a viable growth rate. A two-stage process governs the creation of thin-film diamond: initial nucleation of diamond grains onto the substrate, and growth of those grains into a diamond film [8, 9]. To achieve nucleation, the initial carbon atoms must have an sp^3 basis to attach to and repeat, which can be provided by diamond or another surface with tetrahedral bond formation. The nucleation is needed to ensure enough initial diamond particles are present that the growth rate exceeds the rate at which hydrogen etches the carbon. While hydrogen etches non-diamond carbon faster, it still attacks the diamond formed albeit at a slower rate. Neglecting to seed or prepare the substrate will allow any diamond formed to be etched away more quickly than additional diamond grows to replace it.

Growth conditions are a widely researched aspect of synthetic diamond, but landmark research in 1991 by Bachmann et. al greatly simplified the search for gas ratios resulting in successful growth. By examining

deposition conditions for several dozen experiments over many years, it was found that only select ratios of carbon, hydrogen, and oxygen resulted in diamond growth [3]. This applies to Microwave-Plasma and Plasma Jet Chemical Vapor Deposition techniques, which will be discussed in a later section. Figure 1 represents Bachmann's findings.

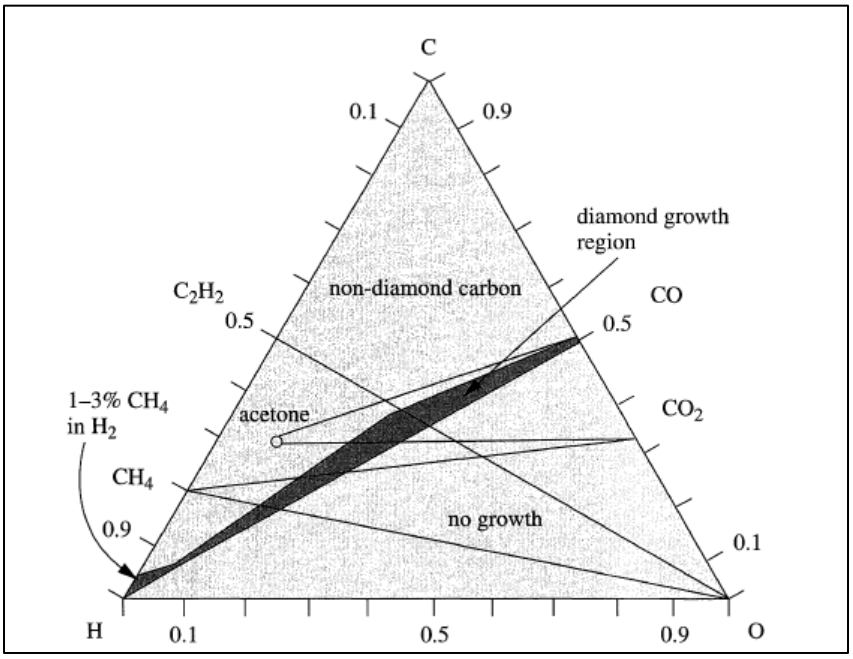

Figure 1 Bachmann's Carbon-Hydrogen-Oxygen gas ratio diagram for diamond growth. The narrow, darkened region shows the ratios of gases which will result in successful polycrystalline diamond deposition. Below this region no growth occurs, whereas above the region carbon deposits in non-diamond form [1]

The diagram greatly narrowed the search for possible diamond-producing process gases; so long as these key elements were present, diamond could be grown. The strict limits of the diamond-producing region in Figure 1 are somewhat indistinct (as some papers weren't specific enough on their process conditions), but some trends are made quite clear, such as the effects of adjusting the percentages of each of these components. It may be seen on the right-hand axis of the chart that oxygen abundance will not allow diamond growth, while carbon abundance results in multiple allotropes of the substance depositing. Non-diamond carbon then chokes out any diamond deposit as the hydrogen etching rate decreases. Within the range of diamond growth, however, exists a compromise: erring towards oxygen abundance

allows finer quality diamond to be grown at a reduced rate, while erring towards carbon abundance allows diamond to be grown faster, but with a greater percentage of sp^2 carbon trapped within its structure.

It may also be seen from these graphs that oxygen is not necessary for diamond growth; it is included in the chart due to being commonly present in deposition process gases, but a carbon-carrier and hydrogen are the two critical species to produce diamond. Methane is often used as the carbon source, diluted in hydrogen gas. Other gases may be added to affect the morphology of the diamond, such as argon. Higher concentrations of argon cause finer-grained diamond growth, at the cost of reduced sp^3 content [10].

For gas ratios within the growth region, process gas temperature and plasma density determine the growth rate to a greater degree than the carbon content does. However, the gas ratios have an even greater effect on the purity than on the growth rate. The diagram applies even for different deposition techniques; Bachmann's group performed supplementary experiments to show the veracity of their diagram, and were successful, although the actual gas species responsible for diamond formation remained an open question between the CH_3* methyl radical and acetylene [11]. Excess atomic hydrogen is vital at each stage of the diamond growth [12]. On the surface of a growing sample, hydrogen caps the dangling bond on each carbon as it attaches in the sp^3 configuration, keeping interfacial carbide layers from forming that could provide greater thermal resistance [13].

Figure 2 shows a commonly accepted CVD diamond deposition cycle. In this process, some carbon may bond in the weaker sp^2 configuration; atomic hydrogen etches away the sp^2 bonded carbon, leaving sp^3 bonded carbon ready to accept the next layer of radicals [14].

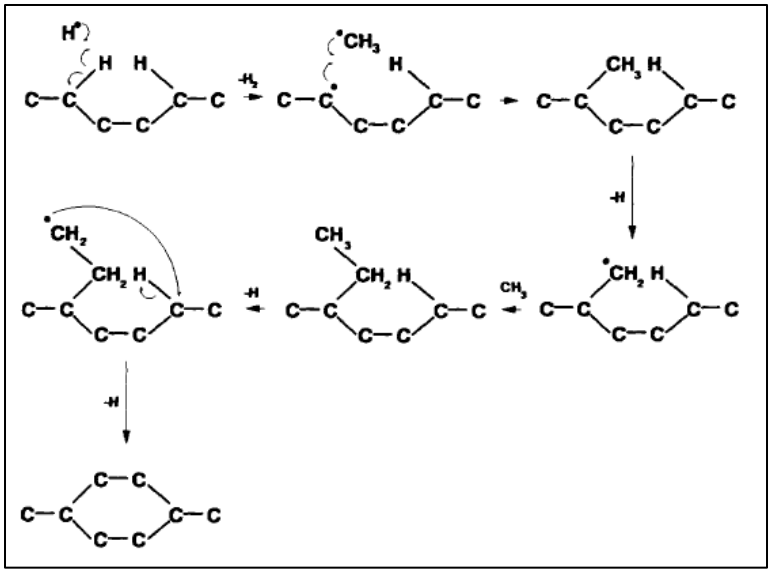

Figure 2 A potential reaction path for atomic diamond growth. A hydrogen atom abstracts a bonded surface hydrogen, creating an open bond on the diamond surface. A methyl radical attaches to the open bond, then a series of additional hydrogen abstractions allow the second carbon to bond to the surface. [6]

2.3 Methods of Diamond Growth

The properties of the finished diamond film are partly determined by the growth method chosen. The common element in all methods is a necessity to activate the process gases, breaking the molecules into the carbon-containing radicals that will create the diamond [1]. Based on the Bachmann Carbon-Hydrogen-Oxygen triangle in Figure 1, the precursor gas must be diluted with a large percentage of hydrogen, so as to ensure sp^3 growth dominates. The broad array of chemical vapor deposition techniques is broken into Hot Filament, Microwave-Plasma, and Plasma Jet. These techniques differ from HPHT and other techniques in that they do not rely on creating thermodynamically stable conditions for the diamond, but instead use gas-phase chemistry.

2.3.1 HFCVD

Hot Filament Chemical Vapor Deposition uses a thin filament, heated up to 2200ºC, to thermally dissociate process gases as they are forced past it. Atomic hydrogen is produced at the filament from hydrogen gas. Activated carbon-containing radicals then diffuse through that region of the chamber;

some bond to the substrate, which is placed millimeters from the filament, as in Figure 3. The advantages of HFCVD are low cost, simplicity, and fairly fast growth rates. However, the resulting diamond may not be pure enough for optical and electronic applications. The filament material, usually Tungsten, gradually breaks down, and contaminates the film on the level of parts per million [15], enough to negatively impact transmissivity and conductivity. The process gases affect the rate of filament breakdown, which forces researchers to take into account the level of oxidation or corrosion likely with each carbon-containing gas.

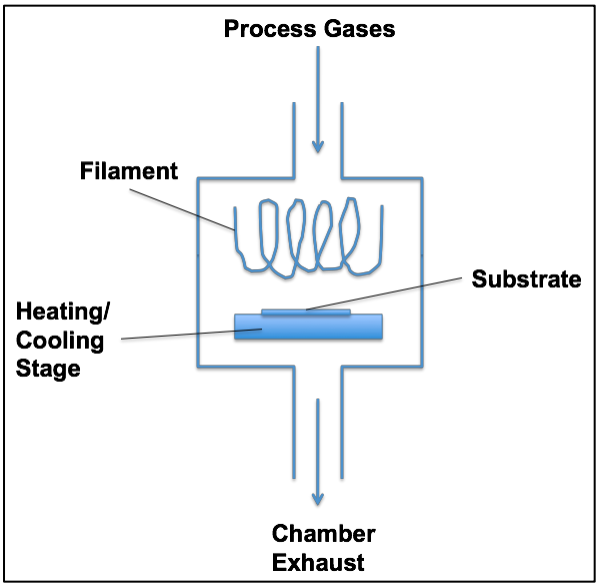

Figure 3 Schematic of Hot-Filament Chemical Vapor Deposition reactor. Process gases enter the chamber and are dissociated by the filament (typically tungsten) that may be heated to 2200°C. The dissociated Carbon diffuses in the chamber and deposits on the prepared substrate surface.

2.3.2 Plasma-Jet CVD

A second way to grow diamond is with a plasma jet or acetylene torch. By using the correct process gases, plasma torches can deposit diamond at a high rate on substrates placed within their jet, as in Figure 4. This is useful for small-area applications of a square centimeter or less. Large-area plasma torches have been developed, but the temperature fluctuation within the jet is an issue for thermal management of the substrate; adequately and evenly cooling a large substrate is challenging. Additionally, the substrate

itself must be carefully chosen due to the sudden increase in temperature at ignition, and sudden decrease at extinguishment. If the substrate does not match the thermal expansion coefficient of the diamond closely enough, the thermal shock may cause the film to detach. While this is a concern for all deposition methods, the temperature rapidly increases when the jet ignites and rapidly decreases when it extinguishes, due to the substrate being in the center of the jet.

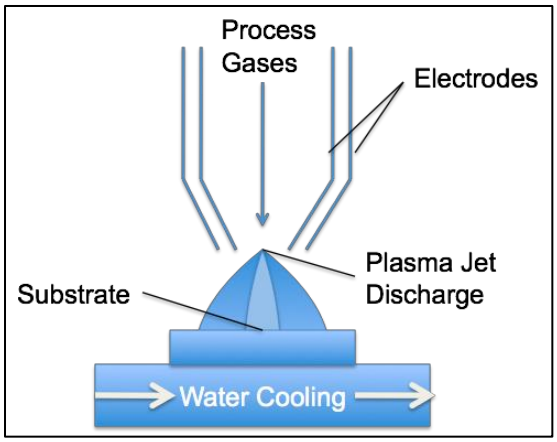

Figure 4 Schematic of Plasma-Jet Chemical Vapor Deposition reactor. Process gases are forced through a nozzle and ignited by electrodes. The sample is placed within the plasma, and the dissociated carbon-containing species bond to the prepared substrate surface.

2.3.3 MPCVD

Microwave Plasma Chemical Vapor Deposition, the method used in this research, is cleaner than HFCVD because it uses microwave energy to dissociate the gas molecules. So long as the chamber walls are kept clean, the diamond will have less non-carbon impurities; this advantage is balanced by additional equipment and operation cost. There is also much more precision afforded with this approach, as the deposition pressure, temperature, process gases, and plasma power can be fine-tuned according to the desired purity, growth rate, and dopant levels [16]. A standing wave of microwave energy ignites plasma from the incoming process gases; the high-energy electrons within the plasma ball dissociate the process gas molecules, creating the atomic hydrogen and methyl radicals needed for growth. The setup is shown in Figure 5. However, unlike molecules dissociated with thermal energy in Hot-Filament reactors,

plasma-decomposed species are ionic. One of the advantages of MWCVD is the existence of these ions. Diamond growth can be slow to establish in CVD, but a technique called Bias-Enhanced Nucleation can use the ions to speed up nucleation and initial growth. BEN involves an electric charge applied to the substrate, readily attracting the oppositely charged radicals. This allows a much denser nucleation layer to form more quickly. This technique is unique to microwave-plasma deposition, and may make it worth the additional cost. Due to the speed of deposition, it is possible for non-diamond carbon to be overgrown by diamond before the hydrogen completely etches it away. For this reason MWCVD films may exhibit additional carbon allotrope and disorder peaks under Raman Spectroscopy as compared to HFCVD films [17].

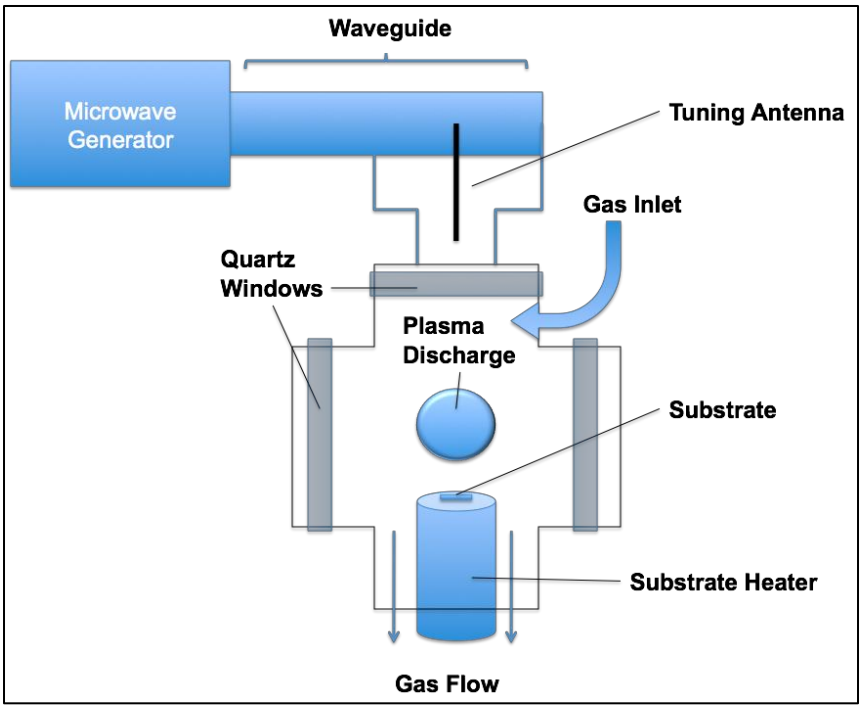

Figure 5 Schematic of Microwave-Plasma Chemical Vapor Deposition reactor. The tuning antenna creates a standing wave that ignites the process gas into plasma. The dissociated carbon-containing species fall onto the substrate below and bond on the prepared substrate surface.

All of these methods require high temperatures, although substantially lower than HPHT methods. Low-temperature deposition is a challenging area of research, but potentially rewarding as it would allow diamond growth directly on temperature-sensitive electronic devices, saving time and money in assembly.

It is more common for diamond to be grown on a substrate, removed from the substrate, then be transferred to its destination.

Growing diamond films requires care in choosing substrates. They must expand and contract with temperature to a comparable degree with diamond, and not change physical properties at deposition temperatures. Silicon is commonly used as it fulfills these requirements, and can easily be etched away post-deposition if free-standing film is required. The top of a substrate must form a carbide layer, especially for materials with different thermal expansion coefficients; this allows the diamond layer to adhere to the substrate, and its absence in materials such as copper may be exploited to grow free-standing films [18, 19]. However, the carbide cannot form too readily, as the mechanical properties of the substrate must be kept intact; this limits the types of metals that can be coated with diamond.

Without of surface treatment, growth is extremely time-intensive as most of the carbon will form sp^2 graphite and be etched away by hydrogen or the diamond nucleation is non-uniform. The growth surface must be prepared to accept carbon atoms in the proper lattice structure. Substrate surfaces can be scored by abrasion with diamond grit; this creates scratches with grooves at the correct angle for carbon linking. It has also been suggested that this allows nucleation due to microdiamonds embedding themselves into the surface. BEN may be used, or a suspension of nanodiamond particles can be adhered to the surface with a dilute polymer. For an untreated surface, less than 10^2 diamond particles may form per square centimeter during a plasma deposition. The treatment methods mentioned may increase the nucleation density to 10^{10} /cm^2 [20].

2.4 Microstructure of Diamond Films

Diamond can be grown in multiple forms, classified by grain size. Single-crystal diamond can be grown through HPHT, and is used for jewelry, cutting tools and scribes, and testing purposes. Most CVD-grown diamond is polycrystalline as surface pretreatments create multiple nucleation sites for faster growth. Depending on the grain size, diamond films are classified as Microcrystalline or Nanocrystalline. The

former have grain sizes on the order of microns, and the latter nanometers. Small grain sizes may be grown by denser initial nucleation and increased nucleation rate [21], or by increasing CH_4 concentration up to 10% [22]. Adjusting the deposition parameters for a reduced growth rate close to the nucleation rate causes the two processes of nucleation and growth to compete for available energy. More nucleates form, thus more grains of shorter length grow. For MCD diamond, fast deposition rate allows grains to compete with each other, some are buried and others grow longer. Reducing the number of grains makes the film harder, as there is less of a chance for sp^2 formation along the grains [23]. Longer grains, however, cause greater surface roughness as a few larger grains form the surface, which will have different orientations. For certain applications such diamond polishing or cutting wheels this is quite helpful. The rough and hard surface doesn't wear down as quickly as other abrasives. Other applications require a smoother surface, such as moving parts in contact or in electronics.

2.5 Properties of Diamond

2.5.1 Mechanical Properties

Diamond exhibits a number of unrivaled attributes due to its strong atomic bonds. The material is useful in different situations based on the dimensions of the diamond. The exceptional hardness of diamond (10 on the Mohs scale, 90GPa) is used for wear-resistant coatings or to make cutting and grinding tools with long lifetimes, from particles or films up to millimeters in thickness or diameter. It has an extremely low coefficient of thermal expansion and low compressibility, which allows it to keep its shape and dimensions even when cutting hard materials. Thicker diamond may be used for scratch-proof windows over sensors, as it is transparent from ultraviolet frequencies to far-infrared.

2.5.2 Thermal Properties

Diamond exhibits remarkable thermal characteristics, especially its conductivity. Due to its very stiff lattice, diamond transmits phonons from regions of high thermal energy at astonishing rates to regions of low thermal energy. As heat conduction in diamond is due to acoustic phonons, they travel at the speed of sound in the material. This value for diamond, 17.5 km/s, is nearly three times that of aluminum and

five times that of gold. Because of its extremely stiff lattice and high melting point, diamond exhibits thermal conductivity several times that of copper, higher than any natural material [16]. Even polycrystalline synthetic diamond may conduct heat as well as single-crystal, although most thin films are only 50-70% as conductive [24]. A low thermal expansion rate means such coatings may be used in high-temperature environments without delamination.

2.6 Diamond films for thermal management

Thermal management of devices is ever more critical, as electronic components continue to shrink and more are placed close together operating at higher and higher speeds. Components lose conductivity and in extreme cases may melt or burn due to overheating. Additional device processing power generates more heat, which limits the number and speed of components. Effective transfer of heat from electronic devices is therefore critical for microelectronics. When designing thermal management systems for electronic components, electrically resistive materials would negate the need for insulating, thermally resistive cladding. Diamond can be semiconductive if doped, but is naturally an insulator because of its large bandgap of 5.4 eV. Its thermal conductivity is due to phonons not electrons, due to its electrically insulating properties.

Phonons, vibrational energy quanta, travel more quickly in stiffer lattice structures; however, impurities or defects in a material, or interfaces between materials, negatively impact efficient heat transfer [25, 26]. An interface acts as a semitransparent mirror, reflecting some phonons while transmitting others.

A boundary between two materials will always exhibit thermal resistance due to mismatched lattice properties or orientation [27, 28]. Grains within a material also negatively impact conductivity, either due to non-diamond carbon or heteroepitaxial grains. Although synthetic films with conductivities approaching that of single-crystal diamond have been grown, thin films of <100 microns in thickness are only 50-70% as conductive at conditions close to room temperature [29]. If the materials are in imperfect physical contact (which is always the case), phonons will be scattered or reflected. This is even more of

an issue for thin films, if they are thinner than the mean free path (MFP) of phonons. The MFP is the average distance a phonon travels before a scattering event [25, 30]. This quantity is temperature-dependent, and varies from 100 microns at close to 0K, to 100 nanometers at room temperature [31]. If the film is sufficiently thicker than the phonon MFP, then the bulk conductivity of the film material is the dominant factor [32]. However, in thin films the additional scattering from surface defects and film impurities has a greater effect on phonons, disrupting their travel and making it more difficult for them to transition to the next material. This increases the temperature discontinuity at the interface, effectively raising the thermal boundary resistance. For thermal applications, the resistance within the film and that across the interface must both be taken into account [25]. Percentile impurity levels can severely lessen the thermal conductivity within a film, and imperfect physical contact at an interface can increase the temperature gradient between two components up to fifteen times [32]. Scattering within a material may be due to a vacancy, interstitial, or isotope. If the phonon wavelength is larger than the physical dimensions of the defect it is described as a point defect. Phonons may scatter elastically when they encounter a vacant site in the lattice structure or a grain boundary; this does not affect their energy but alters their direction [26]. Different scattering events are more common under different conditions. At very low temperatures (less than 200K), grain boundaries are the greatest contributor to thermal resistance [8]. Around 200K, point-defect scattering begins to dominate the thermal resistance. As the temperature increases, phonons are more likely to hit other phonons [33]. However, encounters with other phonons are inelastic, altering their vibrational frequency; these interactions are known as Umklapp processes, and are the primary influence on thermal resistivity at and above room temperature [34].

The interface between diamond and other materials should allow for maximum phonon transmittance, but there is no perfect method to achieve this. Smoother films have greater physical contact but smaller grains, which scatter phonons to a higher degree; fewer grains have lower internal scattering, but result in a rougher surface with reduced physical contact and greater void formation [35]. The film's thickness

does affect the thermal resistance, but the boundary affect is independent of the film dimensions for films thicker than the phonon mean free path [36].

To be at their most effective for heat spreaders and other thermal applications, films must have low impurity levels and few grain boundaries [37]. The latter is due to two reasons: more grain boundaries will scatter phonons, and graphitic carbon has a tendency to form between grains of tetrahedral carbon. This is especially common at higher growth rates, as the diamond grains may close off pockets of sp^2 carbon before they are etched away by hydrogen. Films grown through Chemical Vapor Deposition also exhibit anisotropic thermal characteristics, becoming more conductive layer by layer as they thicken [38]. At the nucleation layer many small grains form from each particle, but grains become fewer and longer as they grow away from the nucleation surface. The longer grains provide an easy conduit for phonons to travel along, perpendicular to the surface. Phonons traveling parallel to the surface, however, must cross multiple grain boundaries. Thus, conductivity across grains for diamond is roughly 90% of conductivity along the grain [8]. In some instances, the earlier layers of a film may be ground away to result in a more thermally conductive film with larger grains. Single-crystal diamond films exhibit primarily isotropic thermal conductivity as the crystal structure is identical and free of grain boundaries in any direction.

2.6.1 Heat Spreaders

One of the uses for diamond films is as interfaces between heat-generating components and heat sinks [10]. Diamond has a low heat capacity, so won't absorb thermal energy from processors and other components. However, due to its high in-plane conductivity, a diamond film on a processor can even out hot spots and transmit heat more evenly to a heat sink. The grain-size differences in MCD and NCD films create different thermal properties; MCD has higher in-plane conductivity but lower across-plane, as the larger grains create a rougher surface. NCD has lower in-plane thermal conductivity due to more grain boundaries, but conducts heat across-plane more easily due to a smoother surface. For heat spreaders, it is desirable to have a mixture of these qualities, thus layered films have been pursued. By

altering gas ratios during deposition, the grain size at the film surface can be altered [10]; two layers of fine-grain NCD separated by a layer of long-grain MCD would be an ideal heat spreader.

2.6.2 Substrates for Electronic Devices

Some applications of diamond films invert the order of layers, with diamond underneath the electronic devices [39]. This is to take advantage of its electrically insulating as well as its thermally conductive properties.

2.7 Measurement Techniques

Diamond films are highly thermally conductive, and are typically grown on thermally conductive substrates. Given how readily heat propagates through the material, it may be challenging to accurately measure the thermal characteristics. Even more challenging to measure is the boundary or interface between a film sample and its substrate, as this may vary with each sample and must be measured indirectly. However, the contribution to the overall thermal resistance may be substantial, and can negatively impact the usefulness of such films for thermal management of small electronic devices [36]. Multiple techniques are available to measure different thermal properties of diamond films; here, several common approaches are described.

2.7.1 Contact

These measurement techniques require the temperature sensing device to be in physical contact with the film or material. This typically means less data processing or analysis to derive the conductivity, as there is some physical quantity being directly measured.

2.7.1.1 3ω/Joule Heating

Metals change their electrical resistance as a function of temperature, and can be evaporated onto surfaces in precise patterns. These characteristics led to development of metal heaters that also act as thermometers. Once a metal line is deposited on the sample surface, an alternating current is passed through it [40]. The frequency of the current ω causes the film surface to heat at double the frequency

[2]. As the metal temperature increases, its resistance oscillates with the frequency of the surface; thus, the resistance oscillation multiplied by the current frequency creates a voltage drop of 3ω. Sensitive equipment can detect this quantity, and relate it to the temperature of the film. This is most effective for isolated films or films on lower-conductivity substrates [41]. This technique may be used on diamond films, and can be used to find diffusivity or conductivity, related by Equation 1,

$$\alpha = \frac{k}{\rho c_p} \tag{1}$$

Where α is the thermal diffusivity, k is the thermal conductivity, ρ its density, and c_p it heat capacity.. This method requires equipment to sputter-coat the sample with the metal pattern, as well as a frequency generator to ensure the alternating current across the wire is a very clean sine wave. To measure the change in voltage of 3ω requires a lock-in amplifier, differential amplifiers, and a digital-to-analog converter. Thus, while the technique can be used to find both the parallel and perpendicular thermal conductivities, the equipment cost required is prohibitive.

2.7.1.2 Thermocouple-based Measurements

Physical thermocouples are the simplest method of measurement, and relatively accurate [42]. These consist of two dissimilar conducting wires joined together at a single point. The temperature of the joint is measured in relation to a cold-junction reference within the readout box. Small thermocouples are necessary for work in the semiconductor field, as large ones may act as heat sinks for small components. It is possible to create a thermocouple on the device itself for testing circuitry or micro-electronics. Sputter or evaporation-deposited heaters and thermocouples are also used to characterize thin films; a mask is used to create a pattern of wires, and silver, gold or platinum is used as the conductive material.

The technique is simple, and thermocouples are inexpensive, but thermocouples may act as a heat sink at the spot being measured. Additionally, slight variations in mounting the device may alter their readings.

2.7.2 Non-Contact

Contact methods entail an additional interface between the sample and the measurement device, whether that be a physical thermocouple or a deposited thin-film heater and sensor. They also may damage the sample, particularly deposition techniques where removal of the device may affect the film. Non-contact methods have their drawbacks, primarily being more complicated than the simplest contact-methods, but are non-destructive in that they do not alter the structure or properties of the film samples examined. Typically non-contact methods measure the thermal diffusivity rather than the conductivity directly, as precise measurement of a temperature gradient is challenging without physical contact [43]. Instead, thermal diffusivity may be measured due to the time delay of heating and cooling response to a pulsed laser.

2.7.2.1 Photodetector and Laser-Flash Analysis

For thicker films, a laser and photodetector pairing can be used to measure the diffusivity of a sample, which relates to the conductivity through the density and heat capacity of a material. In one set-up, an infrared camera is placed behind a sample, and a Nd:YAG laser and photodetector aimed at the front [44]. The photodetector activates the infrared camera once it senses the front surface has begun to heat; the camera then records the temperature rise as a function of time. This does require coating the sample with black paint, to give a high emissivity; it may also be used for free-standing films. A similar method, known as Laser Flash Analysis, can be used for multi-layer films, but only when the film is less thermally conductive than the substrate it is on. Instead of an infrared camera, a photodetector measures the temperature of the top surface as a function of time after a laser pulse to the sample underside. It is challenging to measure very thermally-conductive specimens, and this apparatus can only measure the diffusivity perpendicular to the sample plane. It is accepted that most instruments are too slow for diamond samples, however, so this is less commonly used in typical laboratories [45].

2.7.2.2 Photothermal Methods

Heating a sample with a laser pulse and measuring the thermal decay of the heated surface with a secondary laser takes advantage of the time-delayed cooling of materials. For Thermoreflectance

measurement, the diamond film being measured is coated by gold or another highly heat-conductive and reflective material, and the excited surface molecules alter the reflectance of the sample to a small but quantifiable level [41]. The thermal conductance is found per unit area, from the heat flux generated by the laser, and the film's thickness and heat capacity. Photoacoustic Spectroscopy is a similar method which measures the sound made by gas next to a heated diamond film. As thermal energy leaves a surface by convection, the gas particles next to that surface are energized, creating an acoustic wave. The frequency of this sound may be up to 20 kHz. Optical Beam Deflection takes advantage of the gas molecule movement as well; as the atmosphere at the sample surface heats, its index of diffraction changes from unity, and causes a laser aimed across the surface to change its angle of deflection in a periodic manner as a function of the heating pulse frequency [46]. This method can also measure diffusivity in different directions to check for anisotropic properties. Another method, Photothermal Displacement Spectroscopy, uses one laser to heat the sample surface and a second to examine the surface's thermal expansion; as the surface relaxes, the secondary laser returns to its initial position, and the deflection is related to the diffusivity which can then be used to calculate the conductivity [47]. Each of these methods requires highly sensitive, highly expensive equipment to measure the miniscule scale and extreme speed of the process.

2.7.2.3 Infrared Thermography

The most common non-contact temperature measurement is capturing the energy radiating from an object in the infra-red wavelength. Measuring the thermal energy radiated by an object requires accurate knowledge of that material's emissivity [48]. The sensing instrument may be a pyrometer, which reads the temperature of a single spot, or a camera which captures temperature data over a wider area. Thermal or infrared cameras are like visible-light cameras in several ways, with focal lengths and shutter speeds. However, since they detect light outside the visible spectrum, image processing is unavoidable. The sensors in IR cameras are by necessity digital, and thus have finite resolution. The data from an infrared camera must be processed to create an image. This image will be false-color, as infrared wavelengths are

invisible to the human retina. Temperature values are assigned to a color gradient, but the resolution of the image is limited by the device. Infrared pyrometers also have spot-size limitations, and return a reading that is the average of the temperature for the sensing area.

2.7.2.4 Raman Spectroscopy

Non-contact methods of diamond characterization were developed in part to assist with in situ monitoring of diamond growth; the time necessary to grow useful diamond would be greatly reduced if the film quality could be monitored during growth and the conditions adjusted. One measurement technique that may be used independent of the sample emissivity is Raman Spectroscopy, which measures the vibrations of different atoms and bonds, giving information not just of the elemental makeup but the atomic structure as well [49, 50]. Diamond has a well-defined and well-documented Raman spectra, with a sharp peak at 1332 cm^{-1} and a broad peak at 1530 for synthetic diamond with amorphous carbon [51]. Temperature affects the Raman spectra in two ways: thermal energy added to the system alters the vibrations of individual atoms, increasing the amplitude as heat is added. Additionally, as the material expands according to its thermal expansion coefficient, the distances between individual atoms increase and the bond characteristics alter [52]. An additional consideration for thin-film samples is strain affects between mismatched lattices due to different expansion rates. The position of peaks in the Raman spectra is significantly affected by temperature [48]. Peak position shift is caused by the thermal expansion of the unit cell [53]. This expansion causes the vibrational modes of the bonds to alter [33]. Due to this temperature-dependent effect, Raman spectroscopy has been successfully used for twenty years to measure the temperature of samples during CVD diamond growth [54], and has become widely used to characterize the thermal properties of all carbon allotropes [55-58].

CHAPTER III

PROPOSED WORK

It would be very useful to have a low-cost, effective method of measuring the heat flow through diamond films and particularly between diamond films and substrates. Unfortunately, more accurate methods entail specialized, expensive equipment, along with potentially destructive sample preparation.

This work proposes to test a variety of methods to measure the thermal resistance of CVD diamond thin-films on silicon wafers. Central to all approaches will be the application of the textbook definition of the steady-state (time-independent) form of Fourier's first law of heat conduction.

$$Q_x = -kA\frac{\Delta \mathrm{T}}{\Delta \mathrm{x}} \tag{2}$$

Equation 2 is illustrated in Figure 6 [59]. The goal is to find a low-cost, straightforward, non-destructive method for accurately measuring the temperature drop across a diamond thin-film sample, using equipment common to most labs or inexpensive enough for the majority of labs to purchase.

It will also be necessary to accurately determine the area A across which the heat flux is traveling, the distance x, and the heat transfer rate Q_x. The heat flux will be determined by measuring the power added to the system by the heater. From these quantities, it will be possible to measure the thermal conductivity of diamond thin film samples of different microstructures.

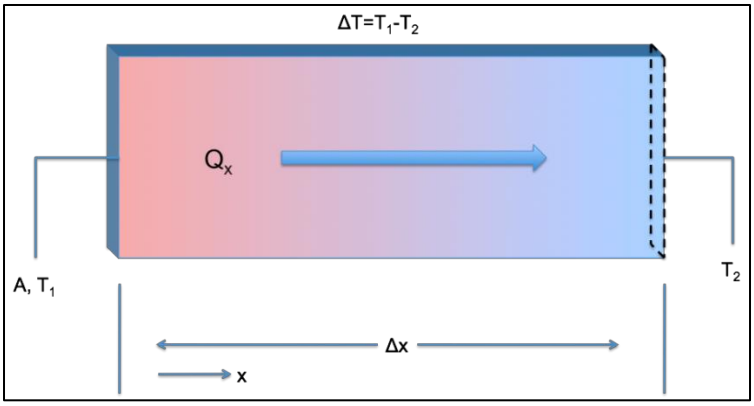

Figure 6 Representation of Fourier's first law of heat conduction (Equation 2). The heat transfer rate Q_x in Watts is the thermal energy moving through a system in one dimension. This quantity is a function of the thermal conductivity k in Watts per meter-Kelvin, the cross-sectional area A in square meters, the distance between the points considered Δx in meters, and the temperature drop between those points ΔT in Kelvin.

CHAPTER IV

EXPERIMENTAL PROCEDURE

4.1 Processing of Diamond Films

Samples were grown on Silicon wafer substrates. These were cleaved to 1" square from 4" diameter wafers, and sonicated in acetone for five minutes then methanol for an additional five minutes. The clean wafers were spin-coated with a 2% PEI dilute polymer solution, then a 25nm diamond particle suspension for seeding with diamond. After drying in open air they were ready for deposition.

The samples were placed in the vacuum chamber. When the chamber is not being used it is backfilled to neutral pressure with nitrogen. This keeps outside air and moisture from leaking in. It is gradually pumped down to the 10^{-3} Torr range with a backing pump. The process gas lines are kept under vacuum between depositions, and so must be purged before each run to ensure process gas purity. The lines are closed, and the chamber may now be pumped to the 10^{-6} Torr regime, to remove impurities and gas molecules that may have adsorbed onto interior surfaces. The turbo-pump is shut off after the desired pressure regime is achieved. The stage is then heated. Process gases are then introduced, starting with Hydrogen. This low-molecular density gas easily ignites into plasma. Heavier gases require more power to start and maintain a plasma. The microwave generator is activated and power increased. The plasma typically ignites at 30 Watts in a very diffuse sphere. Wattage and pressure are increased in unison, and the plasma coalesces into a small sphere roughly 2.5 cm in diameter. Samples over 2.5x2.5 cm^2 are typically not put into the reactor, as diamond film near the corners of the wafer may not be as thick or of

Table 2 Processing Conditions

Sample	Ratio of Ar-H-CH_3 (%)	Deposition Time (hrs)	Stage Temp (ºC)	Pressure (Torr)
21414	60-39-1	4	850	60
30414	85-14-1	3	850	90
81114	0-99-1	5	850	60
90414	60-39-1	3	850	60

good quality . Table 2 shows the deposition conditions for four samples. The sample designations are the dates each sample was initially grown, although additional diamond was grown on each in later depositions. The gas ratios were chosen to create microcrystalline and nanocrystalline diamond films. Increased Argon content causes smaller diamond grains and therefore a smoother film, at the cost of more non-diamond carbon deposited [10].

The stage was heated to 850ºC for each deposition, and the pressure initially brought to 60 Torr. These consistent starting conditions meant differences in thermal conductivity would therefore be due primarily to gas ratios. The increased pressure for sample 30414 was necessary to maintain a plasma in the high-Ar concentration.

After adjusting the power and pressure as desired, additional process gases are introduced. Methane is the carbon-carrier for these experiments, while Argon is used to adjust the ratios of hydrogen and methane as desired. If Argon is being used, it is added before methane. Since the flow rate of Methane will always be 1-5% of the overall flow rate, it is added last. At this point, diamond deposition has begun.

After several hours (depending on the thickness desired), the deposition is halted. The chamber is re-pressurized slowly with nitrogen, and the sample was removed. Post deposition characterization is necessary to confirm diamond growth: weighing, and comparing to pre-deposition weight, allows calculation of the film thickness by multiplying the weight change by accepted density of diamond, 3.51

g/cm^3, times the deposition area of 6.45 cm^2. Raman spectroscopy is then used to ensure the deposited film is diamond (as opposed to graphitic carbon), and that no impurities were present in the chamber.

The sample is then ready for thermal characterization, the main focus of this research. The approach went through multiple iterations, with the primary goal to get reliable and trustworthy measurements that could then be interpreted. The starting point was Fourier's First Law of Heat Conduction. This and the concept of equivalent thermal resistance allow the most important quantities and dimensions to be accounted for easily.

4.2 Setup for Measurement

The core concept of the research apparatus was to physically recreate Fourier's law, specifically the one-dimensional form [59]:

$$q''_x = \frac{Q_x}{A} \tag{3}$$

Equation 3 describes the rate of thermal energy transfer for conduction, in the form of a heat flux q"$_x$ in Watts per square meter. This is a function of the heat rate Q_x and the area A perpendicular to the path.

In cases where the temperature is not time-dependent, the system is defined as being in a steady-state. Thus, the rate equation for heat flux will be a constant, with the temperature linearly dependent on position along the single axis. For a steady-state situation, q"$_x$ W/m^2 may be substituted with Q_x W/A m^2 and Equation 3 re-arranged into Equation 2. When arranged as in Equation 2, the heat rate equation bears remarkable similarity to Ohm's Law, which governs electrical resistivity. This equation describes the movement of electrical charge between regions of high and low electrical potential; under direct current, the circuit is in a steady-state, and the electrical current is the same through each component. Thus, steady-state heat-transfer problems can be examined by creating a thermal circuit. Figure 7 shows a simple resistive electrical circuit, next to an instance of thermal energy transfer. Thermal energy adheres to certain laws, and the transport of this energy is analogous to current flow. A temperature drop

corresponds to electrical potential drop, and electrical and thermal resistance can be compared directly, with σ as the electrical conductivity of a material and k the thermal conductivity . Equation 4 shows this similarity.

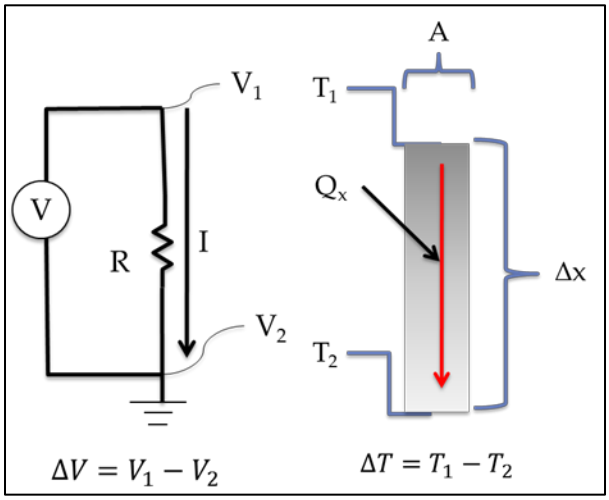

Figure 7 Comparison of Electrical and Thermal systems. Voltage and Temperature gradients are analogous, and heat transfer rate is comparable to current flow.

$$R = \frac{\Delta x}{kA} = \frac{l}{\sigma A} \tag{4}$$

This is of course a simplification of real systems. Not all the thermal energy will travel one-dimensionally through an object. There will be some lateral heat spreading, and energy lost through convection or radiation from the surface. Additionally, interfaces in a thermal system have a much greater effect than in electrical systems. Thermal resistance across an interface or boundary is the reciprocal of the conductance [30, 60], and is defined in Equation 5 as:

$$R_{bd} = \frac{\Delta T}{q} \tag{5}$$

This quantity is the temperature drop ΔT across an interface for a certain heat flux q, and is determined by the bulk properties and surface properties of the materials in contact as well as the interface itself. This resistance is present for every boundary, including grain boundaries within a bulk material.

4.3 Measurement Techniques of Thermal Properties

4.3.1 Contact

The first measurement technique used two k-type thermocouples, placed on the top of the sample next to the edge of the heater, and on the copper block next to the edge of the sample. The placement of thermocouples was based on an assumption made for the experiment: specifically, that heat would travel through the sample one-dimensionally. By matching the heater and sample dimensions as in Figure 8, it was thought that no lateral heat spreading could occur, and a series of parallel thermoclines (planes of identical temperature) would form between the top and bottom surfaces of the sample.

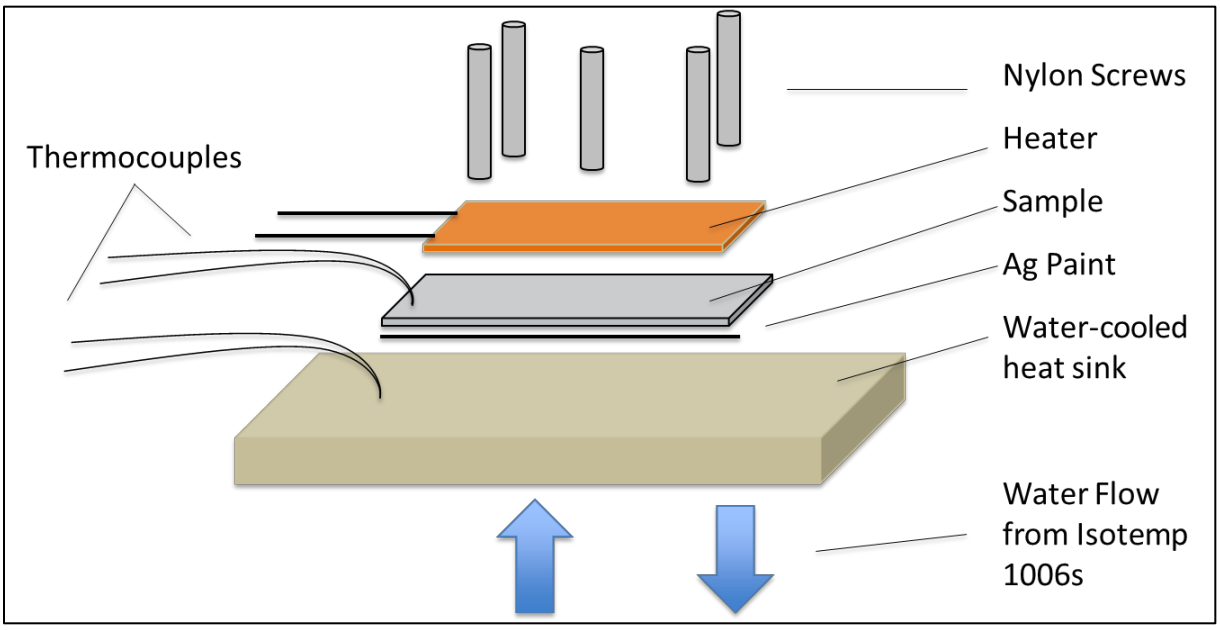

Figure 8 Sample mounting for first iteration

The temperature drop across the sample was measured by thermocouples placed in the same plane as the top and bottom of the thermal gradient across the sample. While it would have been ideal to place the thermocouples directly between the layers, their size made this strategy untenable. Physical contact must be maximized for efficient heat conduction, otherwise air gaps would need to be taken into account. Placing a thermocouple under the sample would have caused the sample to tilt. For a heat sink, a water-cooled brass heat sink was attached to a Fisher Scientific Isotemp 1006S recirculating water chiller. To ensure the chiller maintained a set temperature, a copper tube attached to the lab cold water supply was

immersed in the chiller's small reservoir. A flexible kapton heater was clamped onto the sample by five nylon screws in an x-pattern, to keep maximum surface contact. This combination of heater on one side and chiller on the other established the temperature gradient. Nylon was used both to protect the heater from mechanical damage and to minimize conductive loss from the heater to the screws. Later a piece of glass comparable to the heater dimensions was placed between the heater and screws, as even with five contact points the heater still deformed as it warmed up. An HP 6234a dual-ouput power supply was used to power the heater (maximum output 25V at 0.2A), a Tektronix TDS 1002B oscilloscope to measure the voltage output of the HP, an ammeter to measure the current, and two Omega DP24-T-GN thermocouple meters (accurate to +/- 1°C) to read the thermocouple temperatures.

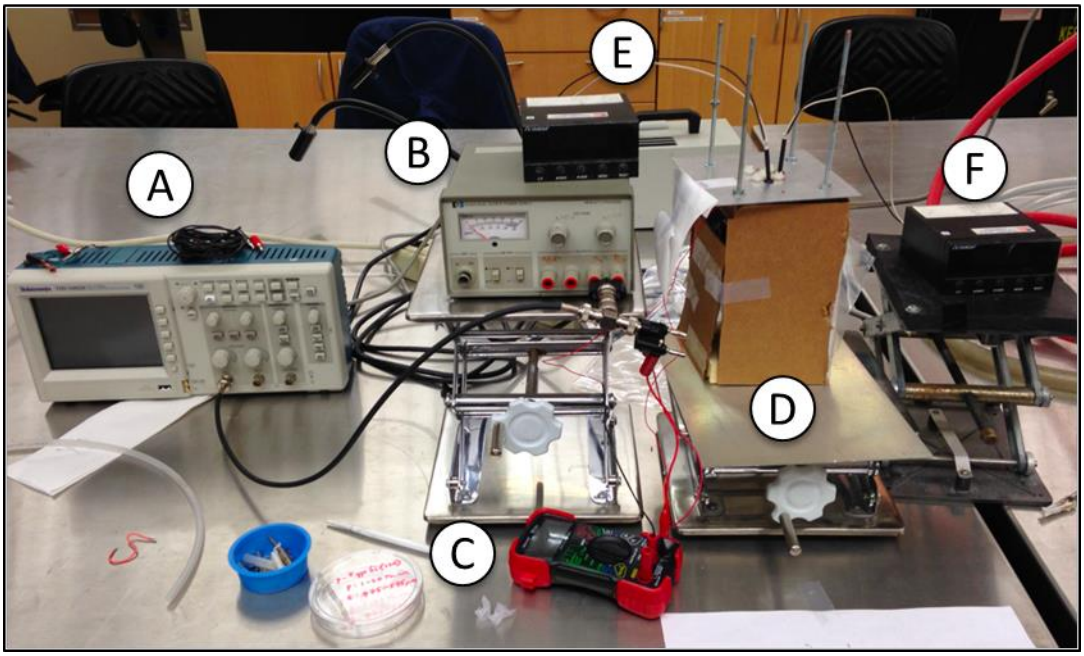

Figure 9 Initial setup, showing (A) oscilloscope for voltage measurement, (B) power supply for heater, (C) ammeter for current measurement, (D) cardboard housing for sample chamber, (E) (F) thermocouple readout boxes for temperature measurement

A cardboard housing was placed around the stage as shown in Figure 9, to minimize convective heat loss. Initially samples were simply clamped under the heater with the screws, and the thermocouples were also kept in place using rubber sheathing on the thermocouples and feeding them through a rubber gasket, to

create friction. The temperature readings from these runs varied greatly; it was observed that the thermocouples were not always in direct contact with the sample and chiller surfaces by the end of the experiment.

Springs were used in an attempt to ensure firm, even pressure on the thermocouples, but readings continued to vary. This may have been due to the thermocouples in use being large enough for the heavy wires to act as heat sinks, which would lower the local temperature of the area being read by the thermocouple. Thus, smaller thermocouples were ordered and mounted differently. Small beads of thermally conductive Pelco silver paint were placed over the thermocouple bead once it was in physical contact with the surface. Once dried, the paint would keep the thermocouple in physical contact, while also increasing the effective area of the bead.

Even with physical clamping, the silicon substrates did not always sit completely flush with the surface of the copper block. Increasing the pressure from the nylon screws would only crack the sample, and so silver paint was also employed to attach the substrate to the cooler. While this would add another thermally resistive layer between the two, it was determined that the paint allowed for more even and repeatable thermal transfer. Additionally in the Thermal Equivalent Circuit analysis, a layer of silver paint is relatively easily accounted for as another resistor in series.

Figure 10 shows the temperature taken with and without the samples adhered to the chiller with silver paint. The steeper slope of 28.05 °C/W denotes a higher thermal resistance between the silicon and the stage, caused by lack of conduction between the silicon wafer and the chiller. As silicon itself is highly thermally conductive, it was expected that reducing the boundary resistance would decrease the overall thermal resistance between the thermocouples. The negatively-sloped line (-6.17 °C/W) is believed due to thermocouple attachment problems, which were still affecting the measurements at this point in the research; however, as it was closer to the expected flat line, it was decided that silver paint would reduce

the thermal resistance between the sample and the heat sink. The other encouraging piece of information was the error bars reduced in size once silver paint was used, indicating more even thermal transfer.

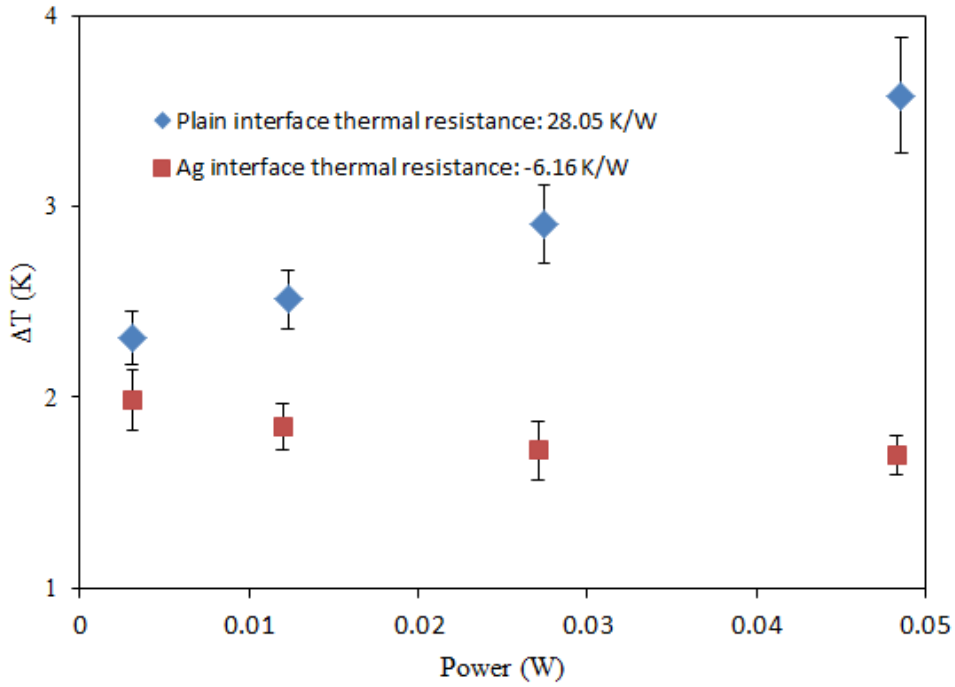

Figure 10 Temperature Drop measured across a silicon wafer with and without silver paint adhering it to the heat sink. The slope constitutes the thermal resistance between two thermocouples. The smaller error bars for the Ag interface show more even heat transfer.

Silver paint was allowed to dry overnight for the sample, and 1-2 hours for the beads on the thermocouples. While the thermocouple readout boxes did not return identical values for the thermocouples, this was deemed acceptable as the quantity of interest was the change in the temperature difference as the heat was increased. However, the temperature range was deemed too narrow for noticeable differences. Both the power supply and heater in use had severe limitations; the power supply could only deliver fifty milliwatts to the heater, leading to extremely narrow power ranges and temperatures. Replacements were sought for each.

A Keithley 228A digital power supply allowing for more precise power levels to the heater (100 mV and 1 mA resolution), and was also capable of higher power output (100 V at 1 A), was used. A new heater was purchased from Birk Manufacturing. The BK-3546-53.0-L12-00 is kapton-encased and measures

1x1 cm^2 with a 53 Ω resistance. It was desired that the new heater be capable of higher power levels, and have a smaller area to increase the watt density, confining the same amount of heat to a smaller area. This would effectively increase the temperature of the sample, without an attendant increase of power input. The 2.5x2.5 cm^2 samples were cleaved to 1x1 cm^2 to maintain homogeny between heater and sample dimensions. The new heater was capable of a maximum temperature of 200°C, well beyond the boundaries of room-temperature experimentation. A BK-3546-53.0-L12-04 heater was also ordered, which is aluminum-backed. This was to test if a stiffer heater with a metal surface would conduct heat to the sample better than kapton only.

However, it was found that the recirculating chiller was responsible for part of the error, due to variations of the building's water supply temperature. To rectify this, it was necessary to add a Peltier cooler to the platform. Attaching the unit to the copper block allowed for more precise cooling, and lowered the stage temperature further than was possible before. The recirculating chiller was still necessary as a Peltier requires a heat sink. A combination of more powerful heater, more effective chiller, and more versatile power source allowed for more precise experimentation. To properly measure the experiment, it was then necessary to purchase a Data Acquisition device (DAQ), as the two readout boxes were not precise enough, and still allowed human error as the readings had to be written down while fluctuating. The purchase of a Keithley 2700 Multimeter / Switch System with a Model 7702 multiplex card allowed use of more thermocouples, and a KUSB-488B USB cable allowed automatic data gathering at the rate of ten points per second; thus, slight variations could be quantified and accounted for.

An ongoing challenge while improving the measurement setup was the mounting and recovery of samples. Leaving the silver paint to dry overnight created a strong bond between the sample and the copper block; while acetone dissolved the paint, it evaporated before penetrating underneath the silicon. Any attempt to pry the substrate off resulted in shattered samples; enough patience and acetone would eventually cause the sample to yield, but this was no longer the case once the Peltier cooler was mounted. Its ceramic surface was rough and porous, and large amounts of acetone were required to dissolve all the

silver paint under the sample. Soaking the cooler in acetone was ruled out, due to unknown effects on the device integrity. Thus, a removable, thermally conductive stage was needed to mount on the Peltier cooler. It was decided to use a piece of brass, cut to the same dimensions as the Peltier. The brass was attached to the Peltier with silver paint and the silicon sample mounted on it; the metal was stiff enough that it could be pried off the Peltier with the silicon intact. This pairing could then be soaked in acetone long enough for the sample to release.

It was found that there was still unreliable data after each adjustment to the apparatus. Small differences in the location of the points being measured and thermocouple mounting at those points caused different temperatures to be recorded. Since only discrete points were being measured, getting accurate measurements of the entire system would be much too time-intensive. It was decided to pursue non-contact measurement techniques to remove variability in sample mounting and temperature measurement.

4.3.2 Non-Contact

4.3.2.1 Infrared

This seemed like a straightforward measurement technique, and could provide much greater detail regarding the heat flow through the system. An ICI 9640 P-Series USB thermal camera was rented to test the usefulness of this approach. Pictures were taken at several power levels. The goal for this was simple comparative analysis; finding the thermoclines within the sample was of great interest, and variation between a piece of silicon and of diamond-coated silicon should theoretically show additional thermal resistance, due to the growth interface. Additionally, by examining the entire set of strata, known values of the properties of silicon and brass could be used to confirm the accuracy of the system and instrument. The instruments, lenses, and software used were powerful and seemingly precise, but therein lay the drawback of this method. To display invisible spectra as visible colors, image processing is unavoidable. The most worrisome possibility was for the software to extrapolate between real values, to enhance the resolution. It was desired that the images retain all of the raw data, but accurately show the limits of the pixel pitch.

Pixel pitch relates the minimum size of resolvable features to the distance from the camera lens, essentially showing the actual area of the object that is captured by each photosensor. As with any analog-to-digital conversion, the "thermal pixel" is the average of the temperature in the given area on the sensor. The software could add pixels by averaging the temperature between two. This was not desired and therefore not used, as the actual values were desired. The images captured were of uncoated silicon wafers and of sample 21414. The heater and chiller were set up identically to the contact-based measurement setup, and the camera positioned from the side to view all the layers at once, shown in Figure 11.

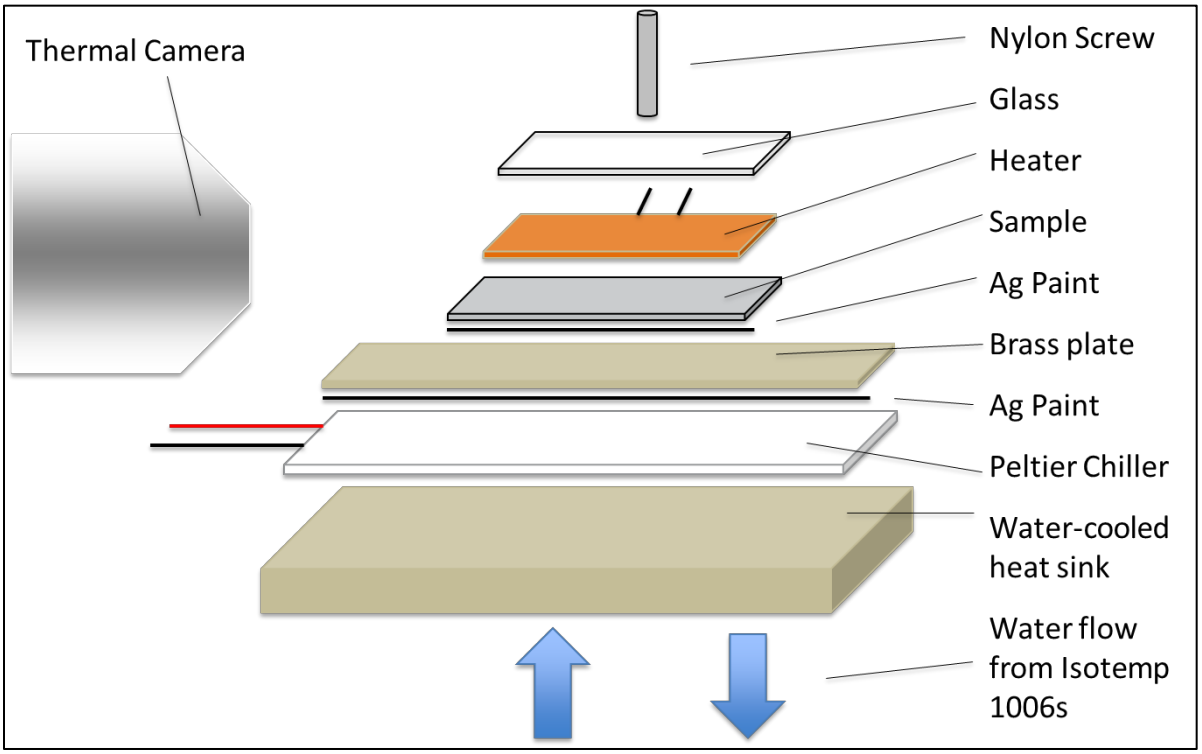

Figure 11 Sample mounting for thermal camera measurements. The camera's field of view covers everything from the nylon screw to the water-cooled block. Only one region at a time may be focused on, however. For the measurements it is focused on the glass, sample and brass plate, the edges of which were lined up.

4.3.2.2 Raman Spectroscopy

It was decided to use the Raman Spectroscopy method to test the thermal conductivity of diamond; specifically, to compare the change in peak position and FWHM to temperature. This experiment was pursued based on the principles of Raman spectroscopy, of measuring the alteration of a laser's phase

when it is reflected off matter. Different materials and bonds absorb and reflect energy in repeatable, distinct ways, allowing elemental makeup to be determined. However, thermal energy excites atoms causing vibrations that stretch and compress bonds, and it was posited that the alteration could be substantial enough for detection. If this were the case, no physical temperature measurement would be needed, as the Raman peak would represent the temperature of the sample. Furthermore, this would allow direct comparisons between samples, in the changes of their thermal properties as a function of growth conditions. It has been shown in other research that the diamond peak is subject to shift with temperature [61]. This shift is accompanied by a change in the FWHM of the peak [62]. As temperature increases, the peak moves to a lower position and the FWHM broadens [63]. This relationship is linear, and each variable's relationship with temperature is linear over short (100K) temperature ranges. The diamond peak shift is -0.0166 cm^{-1}/K [56], while the increase in width was close to 4 cm^{-1} over a 1000K increase, a small quantity compared to other carbon allotropes. This may be due to differences in "occupation number of phonons [56]," as this alters with types of bond, and is also likely due to the stiffness of the diamond lattice. Experiments should show a change in both quantities. Heating was limited to less than 100°C, so as not to damage any components of the microscope or laser. A thermoelectric cooler (powered in reverse to allow heating) was used for temperature adjustment instead of a thin-film heater, as it was large and sturdy enough to provide a stage for mounting samples. However, since a TEC operates by creating a thermal gradient or ΔT, there must still be a steady temperature on one side for the other to experience a constant offset. Thus, the cooling side of the TEC would need to be attached to a heat sink that would keep the temperature constant. This was accomplished by using conductive silver paint to cement the TEC to an metal bracket with a 90-degree bend. The longer part of the bracket then became a fin which extended through a slot in the adjustable Raman stage; a small fan was then positioned to blow along it for the first few experiments, cooling it but keeping it at a constant temperature (verified by a thermocouple); this was eventually dispensed with, however, to allow a greater temperature gradient. The apparatus is shown in Figure 12.

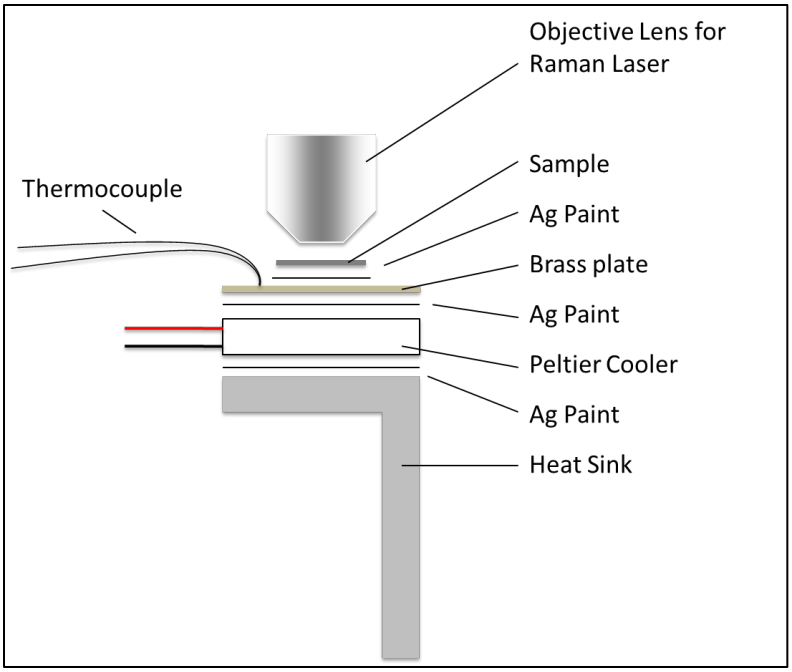

Figure 12 Sample Mounting for Raman Spectroscopy Temperature Measurement. The upper surface of the Peltier is heated, thus the lower surface is cooled when current is passed through the unit. The L-shaped bracket acts as a heat-stabilizing fin. One thermocouple is attached to the brass mounting plate, and the Raman laser is focused on the sample surface.

Local heating from the laser itself must be considered [64]; the power density, especially when focused through a 50x objective, was potentially great enough to heat the sample at the measurement point higher than the average temperature of the sample, causing the shift as a function of temperature to be misread. Some research groups have heated the sample up to 770K using the raman laser itself [64]. However, lower laser power could also result in noisier signal, and so a larger aperture was used to ensure that the laser signal was adequately captured and measured. At the lower laser settings, 140-200 μW of power was directed at the sample, and a 100 μm aperture was used for observation. The collection time was increased from 4 seconds to 20 seconds to reduce signal noise. Later experiments were run with a collection time of 10 seconds as the signal noise was still acceptable. Initial runs were performed on a single-crystal diamond, which is typically used as a calibration standard for the Raman system. The diamond was placed, and the thermocouple glued down 1-2 cm away for each experiment. Due to the very short focal length of both lenses, this was the closest possible mounting distance. An MDX 500 power supply was used for the TEC, and the Keithley 2800A DAQ used to measure the temperature.

Single-crystal diamond and silicon wafer measurements were taken at room temperature. Three to five readings were taken for each set to provide a basis for statistical analysis. Thin-film diamond samples were measured at room temperature and three power levels to the thermoelectric heater. One thermocouple was attached to the surface of thin-film samples for measurement of temperature.

CHAPTER V

RESULTS AND DISCUSSION

5.1 Processing of Diamond Films

Initial characterization of the diamond samples was necessary to ensure the proper material was present. Raman spectroscopy was used to verify the diamond content and film purity. Five spots on the surface of the sample were examined to ensure the film was of regular quality. Figure 13 shows one spectra from each sample compared to a spectra of Single-Crystal Diamond.

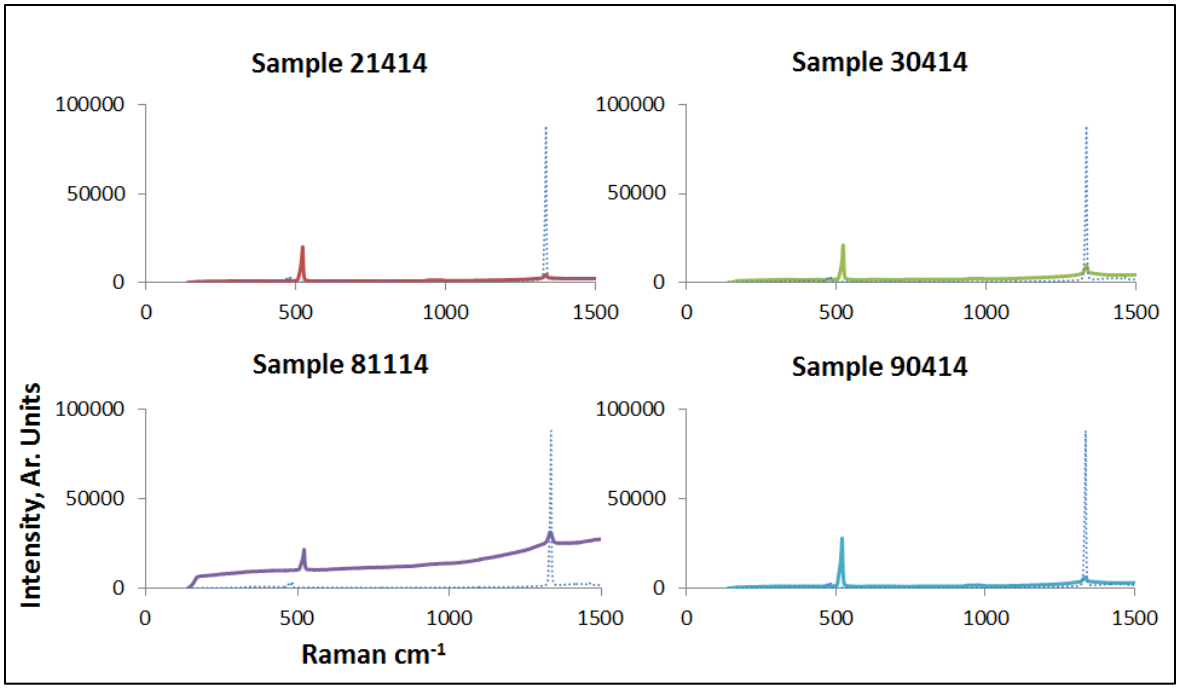

Figure 13 Raman Spectra (Dashed Line) of Single-Crystal Diamond vs Raman Spectra for four Diamond Thin-Film samples. Note silicon peak at 520 cm^{-1}

To determine the film thickness, the wafer with diamond seeding was weighed beforehand on a Mettler Toledo XS 205 balance; five measurements were taken. Post-deposition another set of five weight measurements were taken, and using the density of diamond (3.51 g/cm^3) and the sample dimensions (6.45 cm^2) the average film thickness was determined. Table 3 shows each sample's parameters.

Table 3 Film Characteristics

Sample	Ratio of Ar-H-CH_4 (%)	Deposition Time (hrs)	Stage Temp (C)	Pressure (Torr)	Film Thickness (μ)	Growth Rate (μ/hr)
21414	60-39-1	4	850	60	0.72	0.18
30414	85-14-1	3	850	90	0.895	0.298
81114	0-99-1	5	850	60	1.54	0.308
90414	60-39-1	3	850	60	0.61	0.203

5.2 Thermal properties

5.2.1 Contact

This experiment showed the unsuitability of thermocouples to measure temperature drops. Five thermocouples were attached as in Figure 14, and the temperature drop between each numbered thermocouple and the reference thermocouple recorded. One thermocouple represented in Figure 14B by a triangle was attached to a piece of diamond-coated silicon, and three other thermocouples (a circle, diamond and square) attached to pieces of bare silicon. In theory this should have resulted in identical temperature measurements, so long as the heater underside was isothermal and the glass heated evenly.

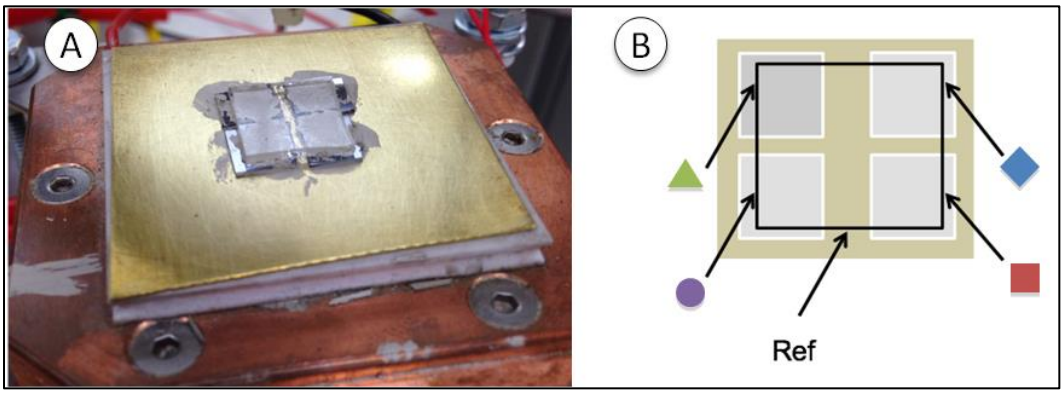

Figure 14 (A) Experiment to test reliability of thermocouples for measuring temperature gradients. (B) Arrangement of thermocouples on setup.

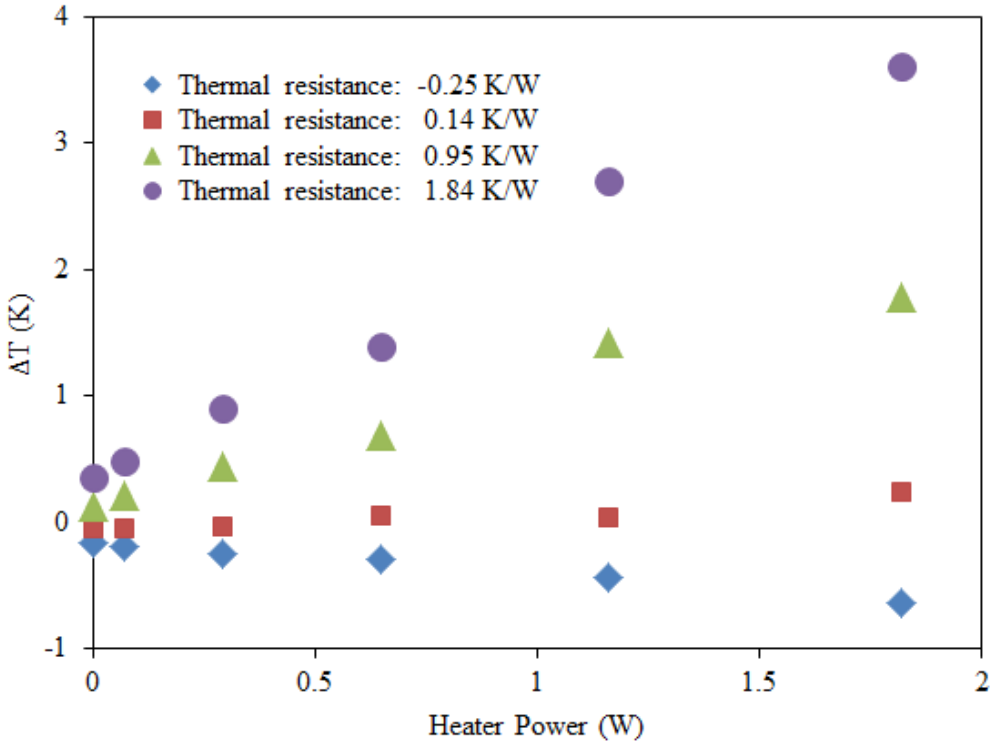

Figure 15: Temperature drops between each thermocouple in Figure 14B and the reference thermocouple.

The widely varying temperatures in Figure 15 showed that even slight mounting variations, and slight inconsistencies of the heater, could produce results that widely varied from expected values. This showed that either the heating was not even (one of the working assumptions), or the differences in how each thermocouple was mounted affected the temperature reading to a high degree. Even heating and lateral heat spreading are critical to this method, so that all points in the same plane parallel to the heater may be assumed isothermal. Thus, taking a temperature measurement in the same plane as the area of interest should give the temperature of that area. This is best understood by referring to the Thermal Equivalent Circuit model in Figure 16 of Figure 14A.

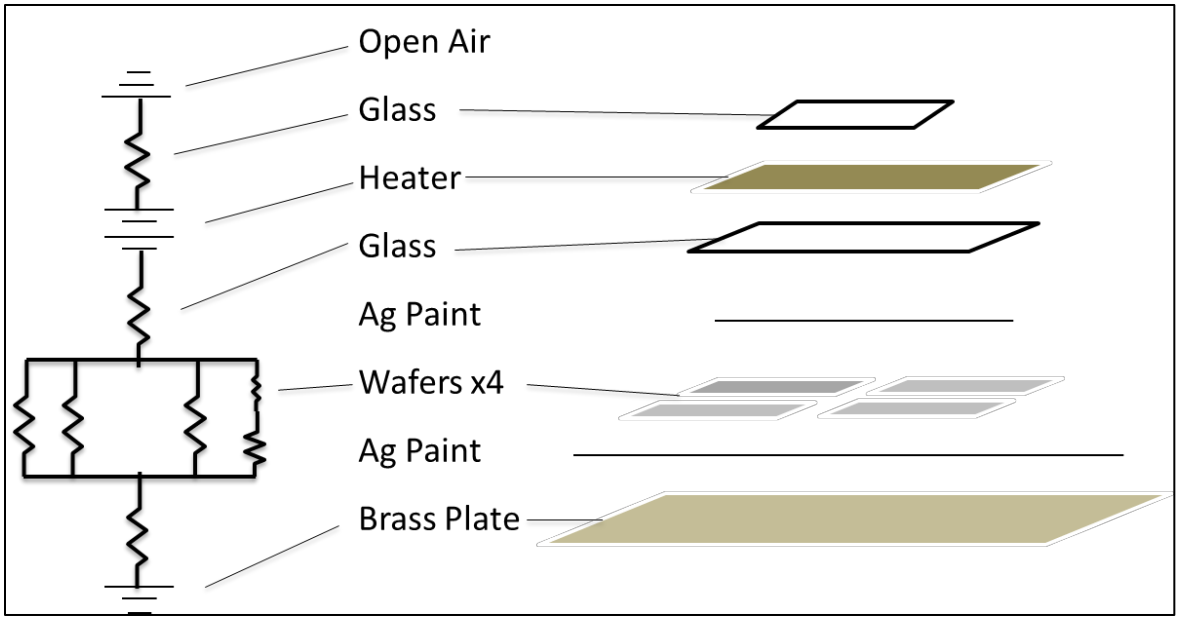

Figure 16 Thermal Equivalent Circuit for Figure 14, showing each layer. The heater acts as the voltage source, and heats the pieces of glass on either side holding it in place. The upper glass loses heat to the surroundings, which act as a heat sink or ground. The bottom glass piece is attached to the samples, one of which is considered as two resistors in series due to its diamond film. These are all adhered to a brass plate, which is the final thermal resistor above the water-cooled heat sink, which is also ground.

The system is composed of multiple elements, each with their own thermal resistances and dimensions. However, by comparison with electrical resistance, even complicated arrangements can be analyzed with relative simplicity. For conduction, each layer is represented as a thermal resistor in a series. Elements of thermal resistance can also be considered parallel. Each layer acts as a resistor, but layers that touch the same surfaces should experience identical temperature drops as resistors in parallel experience identical voltage drops.

Theoretically, the heater should heat evenly, and the Peltier cooler chill evenly, so the heat flux through any point on the setup should be the same. While it would be ideal to measure the temperature at a point between heater and sample, and again between sample and chiller, this was infeasible for two reasons. The physical dimensions of the thermocouple were enough to interrupt the physical contact between each element, reducing the heat conduction of the system. Also, there would be no way to ensure the measured quantity was the temperature of the sample surface, instead of the heater or chiller surface.

Figure 16 shows that the temperature drop measured via thermocouple is unreliable, as it alters based on the points being measured and how each thermocouple is mounted. It was decided that physical contact methods were inherently too inaccurate and too limited for the samples being tested, due to the widely varying temperature drops. Human error would be present in establishing the temperature gradient and in mounting the measurement devices. The amount of silver paint, the position of the thermocouples, and mechanical pressure on the heater, were all critical factors that could change the temperature reading on the level of degrees.

5.2.2 Non-Contact

5.2.2.1 Infrared

Once the thermal pictures were captured with the ICI 9640 via its USB attachment to the lab computer, analysis of the thermographs began. Since each picture contained thousands of data points, only specific areas of interest were examined, beginning with the interfaces between layers. This was more difficult than anticipated, due to uncertainty as to where precisely the interface was located. In false-color images, features that would be obvious in photographs can become indistinct or even disappear dependent on temperature. Some thermal cameras actually overlay temperature data onto a visible-spectrum photograph, but these are typically lower-end devices for home inspection or plant monitoring, and are fairly coarse.

Thus, finding the precise interfaces was difficult. By taking a "strata" of values through the entire stack, however, sharp temperature drops could be matched with material interfaces. Temperature values within the bulk of each layer were fairly simple to sort out; this would show the thermal energy flow through different materials to confirm one-dimensional heat flow, and the thermal properties of each layer. Typically, one pixel covered 20-50 microns, meaning 6-10 pixels across each layer. This was determined by counting the pixels across the known thicknesses of the Silicon wafer and Brass plate, as in Figure 17.

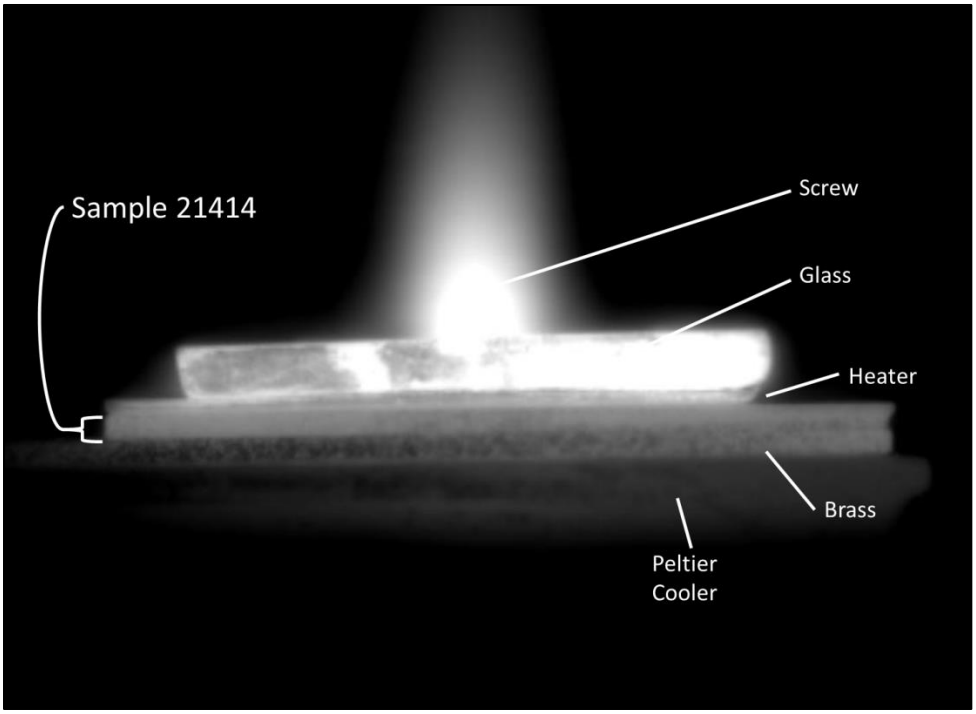

Figure 17 Side view of sample mounting for infrared camera. The edge of sample 21414 is lined up with the edge of the brass plate, to allow the camera to focus on both. The side of the setup facing the camera is sprayed with Arrid to provide a constant emissivity for each layer. The glass piece is somewhat in focus, while the screw is out of focus as it is half a centimeter behind the edge of the glass.

While not ideal for delineating precise thermal gradients, this was enough of a distance to make a reasonable estimate of the temperature drop across a layer. This was not as helpful as was hoped. The temperatures and temperature drops were inconsistent at different portions across the sample width. Figure 18 shows the temperature differences at nine points spaced half a millimeter apart along the top edge of sample 21414 and the bottom edge of the brass plate it was mounted on. The first data point, and the last two, are all at locations where the top of the sample was exposed to air, and thus a lower temperature gradient is expected. However, the remaining points show changes in temperature from 11.2 to 17.4°C. It is difficult to precisely find the interfaces of each layer in the false-color image, but the closest point possible was chosen.

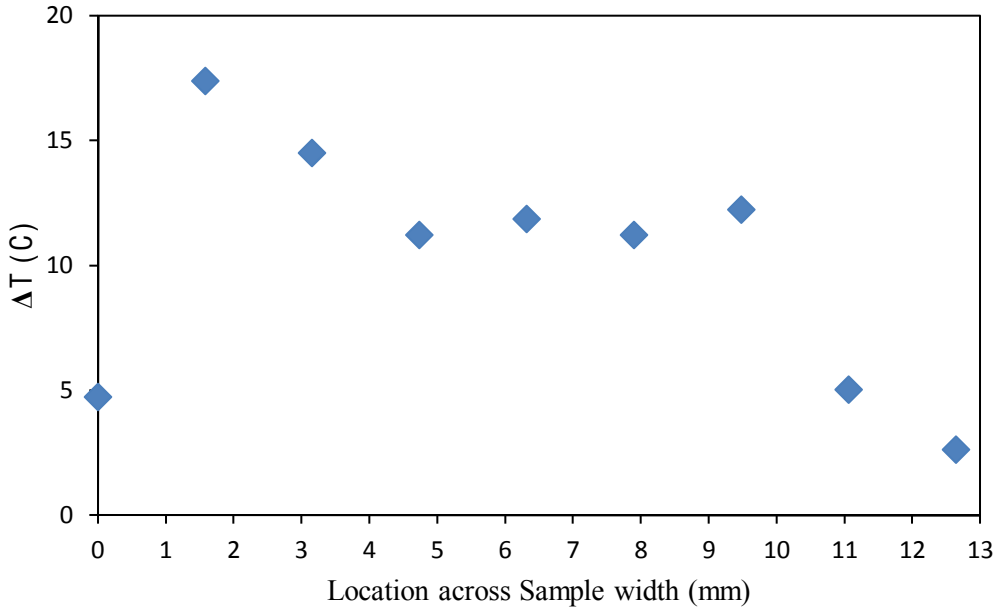

Figure 18 Temperature drop from top of Diamond Sample to bottom of Brass Plate at nine equidistant points across the width of sample 21414 shown in Figure 17.

The discrepancies in temperature drop could be due either to uneven heating or uneven temperature reading; the latter could arise from low emissivity of silicon and brass. Surfaces with low emissivity will not radiate as much thermal energy; thus, non-contact forms of temperature measurement will not read the true surface temperature of objects unless a correction is made. Typically, this is corrected by using a high emissivity coating. According to representatives from ICI, the spray deodorant Arrid Extra-Dry is a good coating, with an emissivity of roughly 0.95, as well as costing very little. This was sprayed multiple times across one side of the setup to make a white powdery coating. One side was left uncoated for comparison. However, even after coating with Arrid, Figure 18 shows the inconsistency of the temperature drops.

After pictures from the side were captured, a picture from above the setup was also captured. This showed the top surface of the glass, as well as giving a roughly perpendicular view of the silicon and brass surfaces. The edge of the silicon next to the brass could be examined in more detail. However, this image revealed a flaw in this characterization approach. The top surface of the glass registered average

temperature 40ºC greater than that of the edge, as shown in Figure 19, calling into question the central assumption of using the side view.

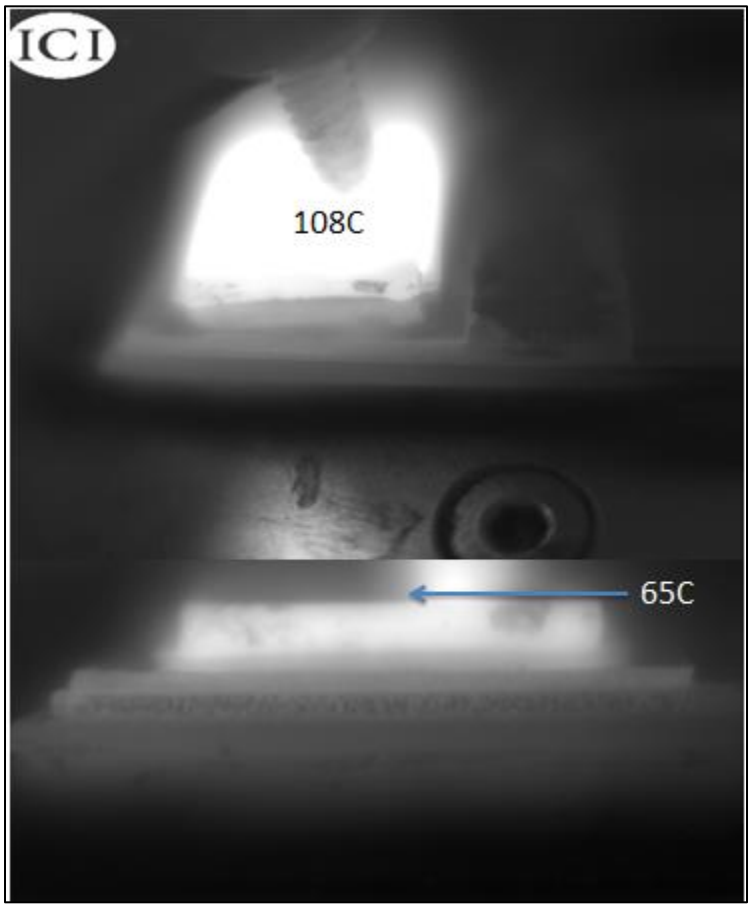

Figure 19 Difference between internal and edge temperature of infrared camera setup.

The temperature of the glass near its center was not equal to the temperature at the edge, therefore the temperature drop across layers at the edge were not representative of temperatures within the system. There was no way to measure the internal temperatures of the system, as thermocouples were too large to fit between the layers. Thus, this method was deemed unusable due to lack of sufficient information regarding internal conditions.

5.2.2.2 Raman Spectroscopy

PeakFit 4.12 was used to examine the data for Silicon, Single-Crystal Diamond, and Diamond Thin Films, and to convert the discrete data points into a continuous curve. Raman peaks may exhibit

distortion due to impurities or instrument error. These distortions negatively impact accurate reading of a peak's position and dimensions; however, by fitting multiple peaks, it is possible to achieve correlation between mathematical and physical spectra. The goal is to find the signature peak of the material and account for instrumentation, defects, impurities, or other experimental factors, using additional smaller peaks that sum to the peaks in the raw data. Extreme care must be taken to fit appropriate functions in relevant locations; enough peaks can exhibit near-perfect correlation but obscure the actual physical data [65].

5.2.2.2.1 Single Crystal Silicon

It was important to first establish the accuracy of the system; this was done by repeated measurements of silicon wafers, as this single-crystal material exhibits a sharp peak at 525 cm^{-1}. The measurements showed the system has a consistent offset and low standard deviation within a set of room-temperature measurements. A Lorentzian curve fits the main peak, and a Gaussian accounts for the background as in Figure 20. The instrumental drift of the silicon peak over several months is shown in Figure 21.

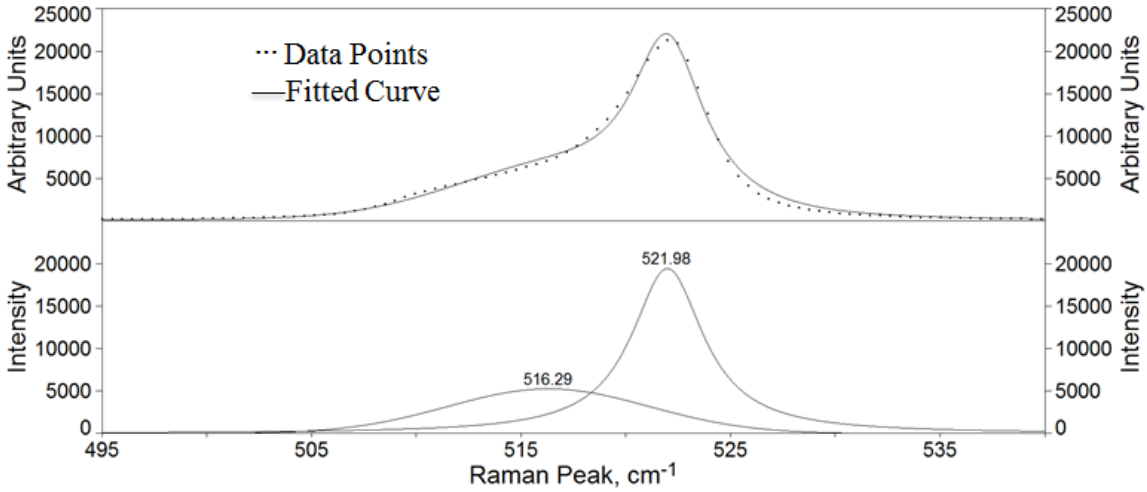

Figure 20 Fitted peak for Silicon wafer, composed of a Gaussian peak at 516.29 cm^{-1} and a Lorentzian peak at 521.98 cm^{-1}. The upper window shows the Raman spectroscopy data points, and the curve fitted to those data points. The r^2 value or correlation factor between the fitted curve and the actual data is 0.9959, or 99.59%. The lower window shows the component curves used.

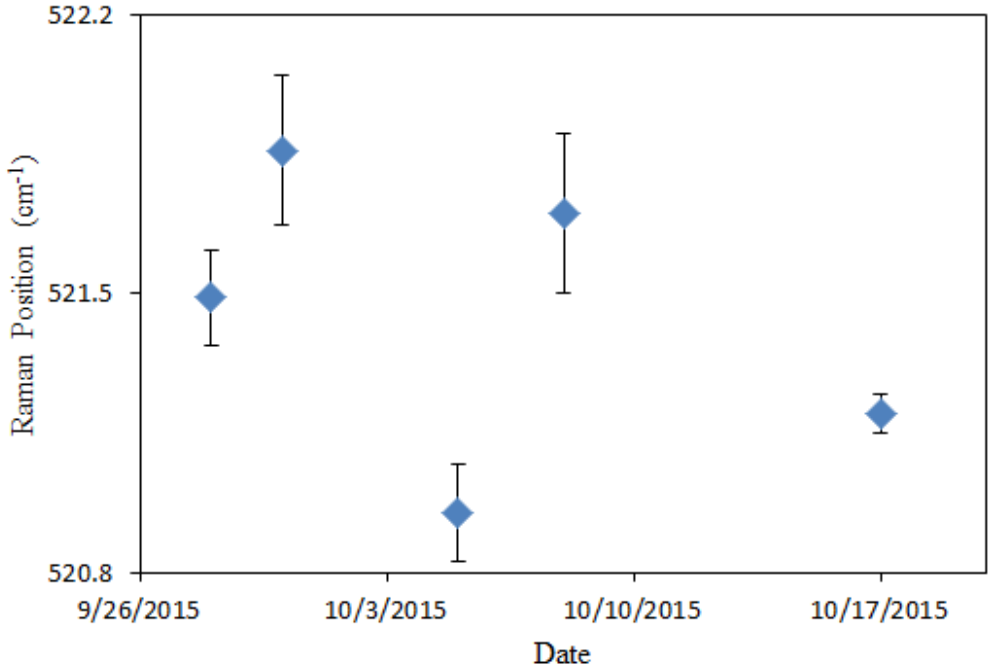

Figure 21 Average Silicon peak positions and standard deviations for room-temperature readings

5.2.2.2.2 Single Crystal Diamond

Standard spectra of common materials are generated by research groups and universities, and published online or in guides. Based on known diamond spectra, one peak was fitted for each single-crystal experiment, which was necessary for calibration and to measure device accuracy. Single-crystal diamond that is fairly pure exhibits a single peak at 1332.5 cm^{-1}; instrumentation effects may shift or distort the peak.

A 1mm-thick Sumitomo standard diamond provided a clean Raman signal, to test the accuracy of the Almega. Sets of five measurements were taken to provide adequate data to calculate statistical deviation; both single-crystal diamond and silicon wafer samples were measured. While diamond generates a Lorentzian peak at 1332.5 cm^{-1}, the instrument itself may add a Gaussian profile to that curve [66, 67]. A Gaussian broadening of the peak may also arise from defects or impurities, and thus can be taken as a measure of the diamond's quality [68]. The data show the peak may shift up to 0.25 cm^{-1} for a given set of

data; the average peak position changes between sets, but this was expected as the internal components re-align each time the apparatus is turned on, creating instrumental drift. Raman spectra standards typically include the shape of the peak, but in general signals from vibrational spectroscopy take on a shape best described by a Lorentzian function. Components of the Raman system, such as the diffraction grating, can add a Gaussian distortion to the peak. It may be more straightforward to use a single Voigt peak, which is a convolution of Gaussian and Lorentzian functions. This is shown in Figure 22. The peaks should be placed in the region of interest manually, but the PeakFit software tweaks the parameters iteratively to achieve the best correlation. The balance between good correlation and physical reality must be kept in mind.

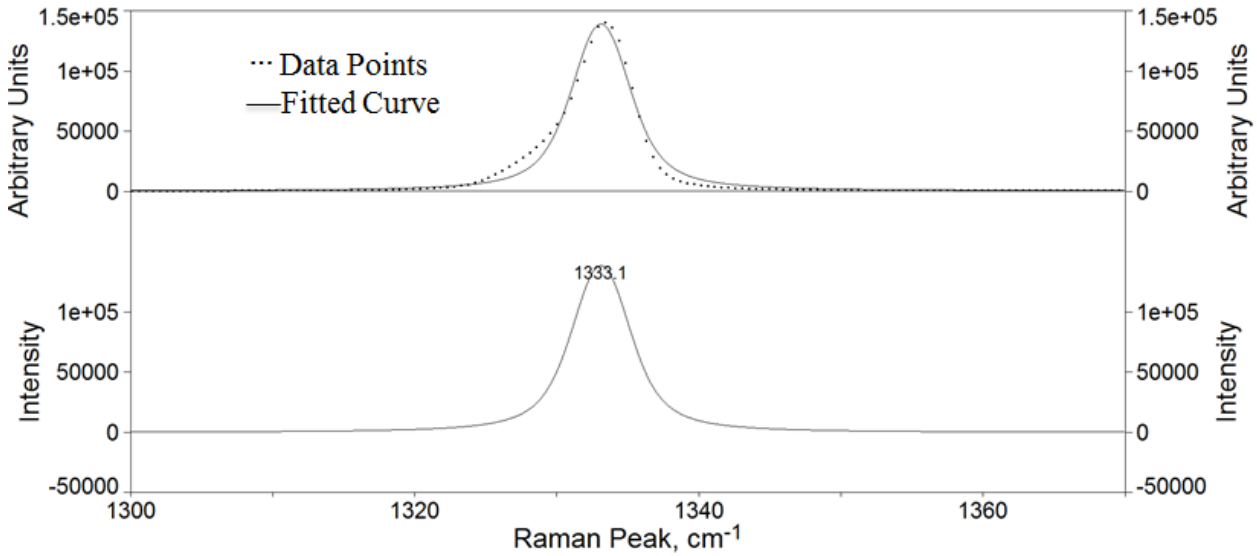

Figure 22 Fitted Voigt Peak at 1333.1 cm^{-1} for Single-Crystal Diamond. The upper window shows the Raman spectroscopy data points, and the curve fitted to those data points. The r^2 value, or correlation factor between the fitted curve and the actual data, is 0.9858 or 98.58%. The lower window shows the component curves used.

The difference in peak position is attributed to instrumental drift; examination in Figure 23 of single-crystal diamond peaks stretching back several years shows variation of central diamond peak between 1331.97 cm^{-1} and 1335.78 cm^{-1} from 2011 to 2015. The standard deviations for each set of data are consistent with those for Silicon measurements, thus the system is accurate to 0.25 cm^{-1}.

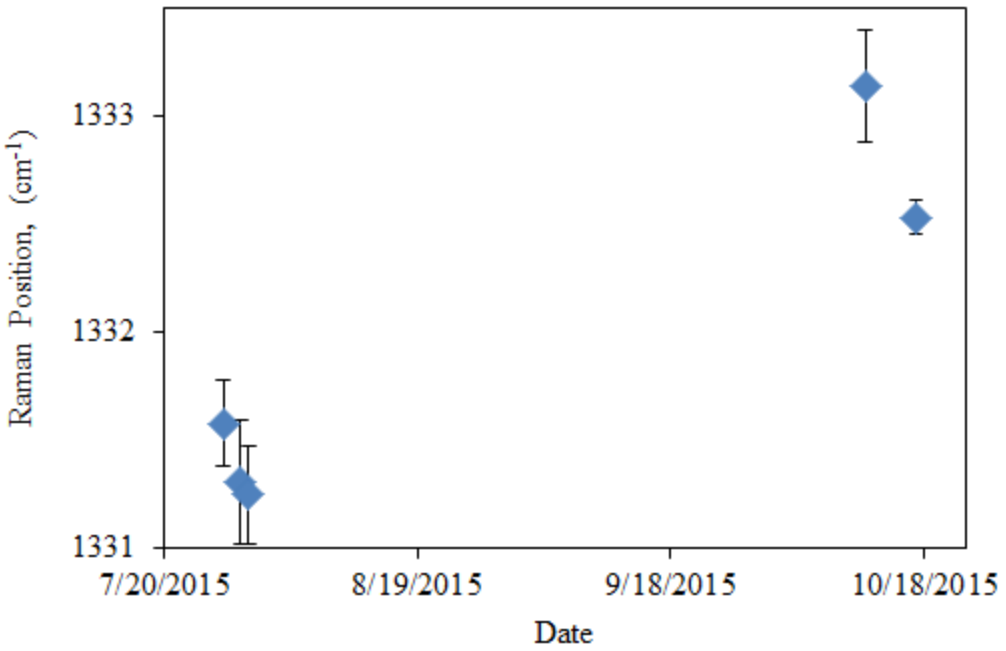

Figure 23 Average Single-Crystal Diamond peak positions and standard deviations for room-temperature readings

The laser's penetration depth was a concern, particularly for confirming the thermal response of the diamond peak for a single crystal. If the laser was penetrating through the diamond completely, then the substrate could be responsible for altering the spectra, both at room temperature and while being heated. The single-crystal standard was placed on a silicon piece; at room temperature and under heating, no silicon peak was evident. This shows the laser did not penetrate the Single-Crystal Diamond, thus heating effects from the Silicon would not have altered the diamond peak position or width.

5.2.2.2.3 Diamond-Coated Silicon

Unlike Single-Crystal Diamond, CVD diamond may exhibit many peaks dependent on impurities, growth and processing conditions, and physical and thermal stresses. Peak fitting for diamond films is less straightforward, as often the signal is noisier and the peak intensity will be greatly reduced. The polycrystalline film may have non-diamond carbon that creates disorder, and Raman signal of the substrate will leak through dependent on the film thickness. With so many considerations that affect the peak position and shape, peak fitting becomes "as much an art as a science [65]."

From the CVD data, the diamond thin films exhibit much less pristine signal, with Disordered carbon (a broad, low peak anywhere from 1310 to 1450 cm^{-1}) and Graphitic carbon (a broad peak centered between 1520 and 1610 cm^{-1}) bands in evidence. Furthermore, the Silicon peak resulting from the substrate is in some cases stronger than the diamond peak, and is always better defined. In such cases, more data processing must be done but carefully for the reasons outlined above. It may be beneficial to consider the diamond peak in isolation, by sectioning the spectra the program will consider. This should not be done if it is believed that peaks beyond the section chosen are wide enough to affect the peak in question. However, a section from 1250 to 1400 cm^{-1} was deemed wide enough to include the most typical CVD peaks, a Lorentzian function to describe the diamond and a Gaussian function to account for disorder or impurities [69]. This section consisted of the peak and "tails" on either end, but the tails showed a marked slope. It was decided to subtract a baseline, normalizing selected data points to a linear horizontal axis. Since the tails already exhibited linear behavior, applying a baseline subtraction was straightforward. Peaks used for fitting were one Voigt profile at the main peak, and a Gauss profile low and off-center to account for the background, as in Figure 24.

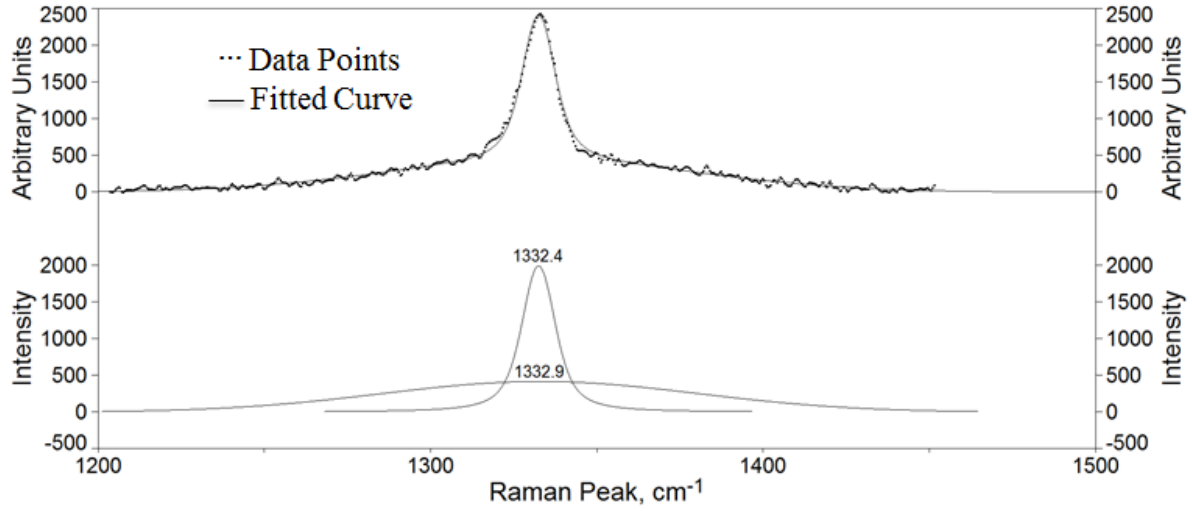

Figure 24 Fitted peak for Diamond-Coated Silicon wafer, composed of a Gaussian peak at 1332.9 cm^{-1} and a Voigt peak at 1332.4 cm^{-1}. The upper window shows the Raman spectroscopy data points, and the curve fitted to those data points. The r^2 value, or correlation factor between the fitted curve and the actual data, is 0.9924 or 99.24%. The lower window shows the component curves used.

The results are tabulated in Table 4 and visualized in Figure 25. The correlation values for each peak are included, to relate the degree to which the mathematical curve used for the position value describes the measured peak data.

Table 4 Effect of temperature on diamond peak of thin-film samples.

Sample	Peaks	Correlation	Temperature	Sample	Peaks	Correlation	Temperature
21414	1332.45	0.9926	22.4	30414	1332.68	0.989	21.6
	1332.11	0.9922	32.2		1332.51	0.9874	32.6
	1332.19	0.9941	39.6		1332.3	0.9874	42.2
	1331.8	0.9932	51.8		1332.48	0.9892	53.4
81114	1332.48	0.9907	22	90414	1333.02	0.9784	22.6
	1332.38	0.9877	32.44		1332.81	0.9781	32.6
	1332.25	0.9911	42.1		1332.7	0.9778	42.1
	1332.09	0.9905	53		1332.29	0.9794	53

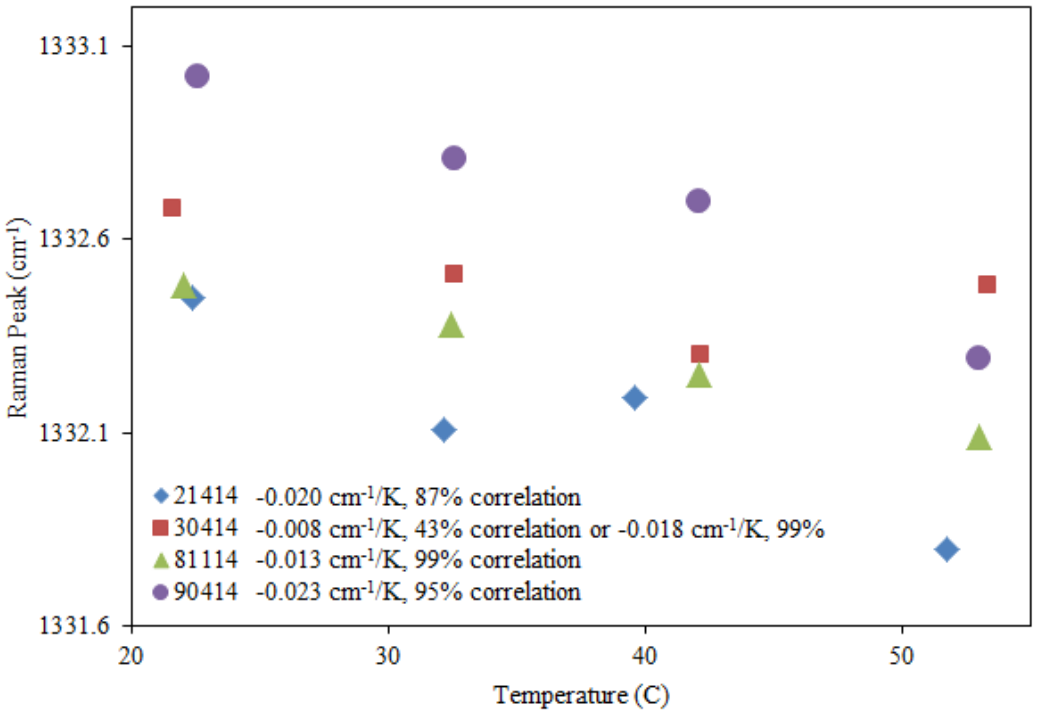

Figure 25 Thermal response of the diamond peak for diamond thin-film samples. Sample 30414 has two slopes due to the final data point exhibiting unexpected behavior. The first value of -0.008 cm^{-1}/K is the best-fit slope for all four data points, while the second value of -0.018 cm^{-1}/K is the slope for the first three data points only.

Multiple samples were tested, and while each exhibited unique slopes, the values were consistent with published data [35, 36, 56]. As the system is only accurate to 0.25 cm^{-1}, temperature differences of 10C

minimum were necessary for reliable readings. Of note is sample 30414; the highest-temperature peak reading did not follow the trend but seems to have regressed. This is possibly due to variations in film thickness at different measurement spots, or local heating and cooling effects. The silicon peaks for each spectra were also examined in Table 5 and Figure 26, as it was expected they would shift position as well [70, 71].

Table 5 Effect of temperature on silicon peak of thin-film samples.

Sample	Peaks	Correlation	Temperature	Sample	Peaks	Correlation	Temperature
21414	521.87	0.9958	22.4	30414	521.9	0.9938	21.6
	521.43	0.996	32.2		521.52	0.9856	32.6
	521.1	0.9964	39.6		521.49	0.9895	42.2
	520.71	0.9959	51.8		521.25	0.9925	53.4
81114	521.82	0.9966	22	90414	522.1	0.9959	22.6
	521.92	0.9962	32.44		521.96	0.9956	32.6
	521.44	0.9962	42.1		521.73	0.996	42.1
	521.31	0.9963	53		521.21	0.9903	53

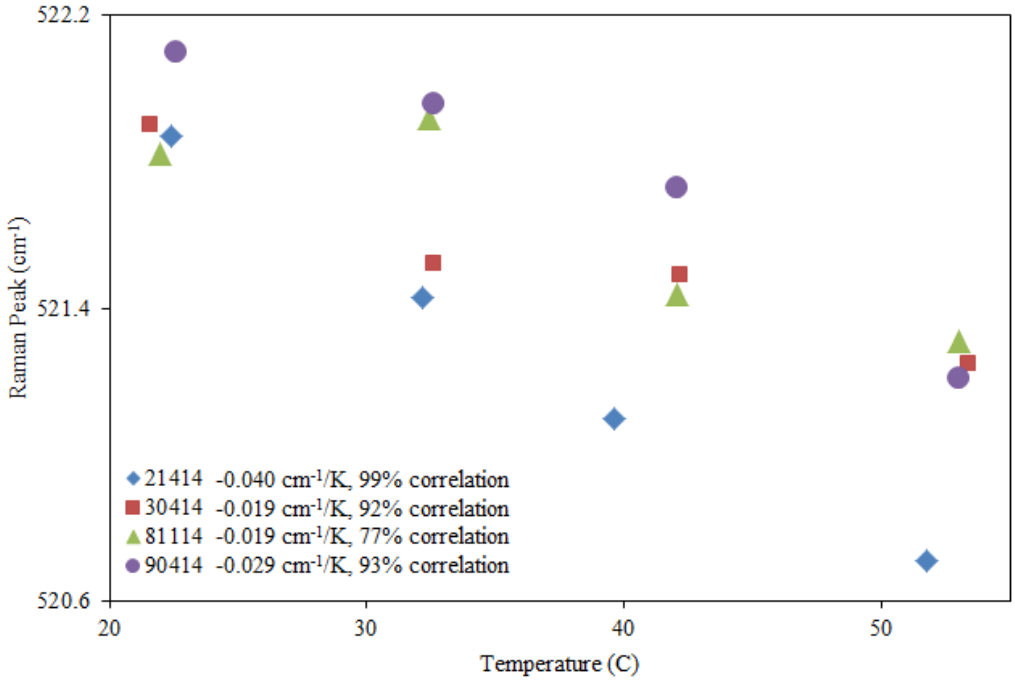

Figure 26 Thermal response of the silicon peak for several diamond thin-film samples

These values were different for each sample, likely due to differences in the interface and film characteristics. For example, variations in film thickness could cause the silicon signal to be altered

slightly based on measurement location. This could be pursued further by comparing the temperature response for Silicon and Diamond peaks of different samples. Given that each film exhibits a unique Raman response to temperature increase, and that there is consistency between runs, Raman spectroscopy is the most promising approach for determining the temperature of a sample with minimal human error.

CHAPTER VI

CONCLUSIONS

Several methods were attempted to measure the thermal characteristics of diamond thin-films grown on silicon wafers. The conclusions drawn were:

1. Seemingly simpler methods are prone to human error in experimental setup and inaccuracy in data gathering. The contact-based methods, using thermocouples and heaters, revealed the challenges of applying Fourier's law to model real systems. It must be assumed that no heat escapes the system except by flowing through it, and that the energy passing through the system and the resultant temperature gradient can be measured accurately. Even so, useful knowledge was gained from this approach. Thermocouples allowed quick feedback on adjustments made to the system, as it was obvious when a change made temperature measurements more accurate or consistent between data sets. Using silver paint as both an adhesive and thermal interface, and mounting samples on a removable plate, were both strategies employed for later experimental setups. It was decided the human error in setting up and measuring the system was too great, however, in that mounting samples and thermocouples involved many possible inaccuracies.
2. The first non-contact method, infrared thermography, exhibited a further limitation, namely expecting heat to flow evenly in real systems as it does in ideal scenarios. The temperature profiles at the edge of the system were inconsistent, and didn't correspond to the temperature within the system. Coatings were used to account for the emissivity differences of each material;

but it was shown that applying the coatings added error similar to that of mounting thermocouples. The other limitations were the physical dimensions of the setup and the focal lengths of the lenses, as well as the cost of the system and the resolution of the device.

3. Raman spectroscopy is able to measure thermal characteristics in a repeatable and accurate manner, as there is little possible variation in setup and less in data gathering. Using a single thermocouple reduces the possible error. Using the Raman system meant taking advantage of equipment already owned, and of a well-documented method of measuring temperature. It was necessary to determine the accuracy of the system, but once this was done the samples could be characterized. The advantage for Raman was the minimization of human error, as the measurement itself was taken independently of human input. As this technique is dependent on average bond length between atoms, it is thought to give the most accurate representation of the actual temperature, as there are no interfacial or emissive resistances present. Nevertheless there are drawbacks. Deriving the interfacial effects still presents a challenge, as the Raman laser penetrates the film. Local heating from the laser may also play a role in altering the signal; describing this effect will be pursued in future research. Based on the data shown in the previous section, Raman spectroscopy may be used to determine the temperature of individual thin films. It may also be used to determine the temperature of the silicon underneath, as both peaks shift but dissimilarly. There is a good degree of consistency among different Raman measurements: both Silicon and Single-Crystal Diamond peaks typically exhibited variance of 0.25 cm^{-1}, thermal response slopes for Diamond Films were close to published values, and Silicon and diamond show distinct thermal responses.

Attempting to re-create textbook scenarios reveals the inherent assumptions made in ideal systems. In certain systems, such as optical or electrical, the inefficiencies of real components may have a negligible impact on measurement. However, thermal systems exhibit stark differences between the page and the bench. This may be due to challenges posed by the films and measurement techniques. Fourier's law

assumes accurate measurement and being able to account for all heat flow; both are difficult to do in reality. However, pursuit of the perfect is the only way to reach scientific breakthroughs. While the research has shifted its initial focus, each measurement technique came closer to achieving the goal of quantifying the thermal properties of diamond-coated silicon films.

CHAPTER VII

FUTURE WORK

Several more questions remain, which will be pursued under PhD work. Pursuing the thermal boundary resistance between diamond and Silicon is of primary interest. This is tied with seeking low-temperature deposition to grow diamond directly on electronic devices; if low-temperature deposition can be harnessed, and the conditions optimized for low thermal boundary resistance, it will be possible to create electronics that run at higher speeds and power. To accomplish those goals, the principles of this thesis must be applied to a range of samples and the growth conditions linked to the thermal boundary resistance of different films.

REFERENCES

[1] P. W. May, "Diamond thin films: a 21st-century material," *Philosophical Transactions of the Royal Society of London Series a-Mathematical Physical and Engineering Sciences,* vol. 358, pp. 473-495, Jan 2000.

[2] F. Volklein and T. Starz, "Thermal conductivity of thin films-experimental methods and theoretical interpretation," in *XVI ICT '97. Proceedings ICT'97. 16th International Conference on Thermoelectrics (Cat. No.97TH8291)*, Place of Publication: New York, NY, USA; Dresden, Germany. Country of Publication: USA.

[3] P. K. Bachmann, D. Leers, and H. Lydtin, "TOWARDS A GENERAL CONCEPT OF DIAMOND CHEMICAL VAPOR-DEPOSITION," *Diamond and Related Materials,* vol. 1, pp. 1-12, Aug 1991.

[4] S. Tennant, "On the Nature of the Diamond," *Philosophical transactions of the Royal Society of London,* vol. 87, pp. 123-127, 1797.

[5] S. Ferro, "Synthesis of diamond," *Journal of Materials Chemistry,* vol. 12, pp. 2843-2855, 2002.

[6] M. N. R. Ashfold, P. W. May, C. A. Rego, and N. M. Everitt, "THIN-FILM DIAMOND BY CHEMICAL-VAPOR-DEPOSITION METHODS," *Chemical Society Reviews,* vol. 23, pp. 21-30, Feb 1994.

[7] V. V. Danilenko, "On the history of the discovery of nanodiamond synthesis," *Physics of the Solid State,* vol. 46, pp. 595-599, 2004.

[8] J. E. Graebner, S. Jin, J. A. Herb, and C. F. Gardinier, "LOCAL THERMAL-CONDUCTIVITY IN CHEMICAL-VAPOR-DEPOSITED DIAMOND," *Journal of Applied Physics,* vol. 76, pp. 1552-1556, Aug 1994.

[9] H. T. Ye, C. Q. Sun, P. Hing, H. Xie, S. Zhang, and J. Wei, "Nucleation and growth dynamics of diamond films by microwave plasma-enhanced chemical vapor deposition (MPECVD)," *Surface & Coatings Technology,* vol. 123, pp. 129-133, Jan 2000.

[10] N. Govindaraju, C. Kane, and R. N. Singh, "Processing of multilayer microcrystalline and nanocrystalline diamond thin films using Ar-rich microwave plasmas," *Journal of Materials Research,* vol. 26, pp. 3072-3082, Dec 2011.

[11] M. I. Heggie, G. Jungnickel, and C. D. Latham, "The theory of CVD diamond growth," *Diamond and Related Materials,* vol. 5, pp. 236-241, Apr 1996.

[12] W. Piekarczyk, R. Messier, R. Roy, and C. Engdahl, "DIAMOND DEPOSITION BY CHEMICAL VAPOR TRANSPORT WITH HYDROGEN IN A CLOSED SYSTEM," *Journal of Crystal Growth,* vol. 106, pp. 279-293, Nov 1990.

[13] S. Jiao, A. Sumant, M. A. Kirk, D. M. Gruen, A. R. Krauss, and O. Auciello, "Microstructure of ultrananocrystalline diamond films grown by microwave Ar-CH4 plasma chemical vapor deposition with or without added H-2," *Journal of Applied Physics,* vol. 90, pp. 118-122, Jul 2001.

[14] W. Piekarczyk and W. A. Yarbrough, "APPLICATION OF THERMODYNAMICS TO THE EXAMINATION OF THE DIAMOND CVD PROCESS .2. A MODEL OF DIAMOND DEPOSITION PROCESS FROM HYDROCARBON HYDROGEN MIXTURES," *Journal of Crystal Growth*, vol. 108, pp. 583-597, Feb 1991.

[15] D. T. Morelli, T. M. Hartnett, and C. J. Robinson, "PHONON-DEFECT SCATTERING IN HIGH THERMAL-CONDUCTIVITY DIAMOND FILMS," *Applied Physics Letters*, vol. 59, pp. 2112-2114, Oct 1991.

[16] D. Das and R. N. Singh, "A review of nucleation, growth and low temperature synthesis of diamond thin films," *International Materials Reviews*, vol. 52, pp. 29-64, Jan 2007.

[17] M. A. Dar, Y. S. Kim, S. C. Ansari, H. I. Kim, G. Khang, C. Van Chiem, *et al.*, "Comparative study of diamond films grown on silicon substrate using microwave plasma chemical vapor deposition and hot-filament chemical vapor deposition technique," *Korean Journal of Chemical Engineering*, vol. 22, pp. 770-773, Sep 2005.

[18] Y. Q. Fu, H. J. Du, and C. Q. Sun, "Interfacial structure, residual stress and adhesion of diamond coatings deposited on titanium," *Thin Solid Films*, vol. 424, pp. 107-114, Jan 2003.

[19] G. S. Ristić, Ž. D. Bogdanov, S. Zec, N. Romčević, Z. Dohčević-Mitrović, and Š. S. Miljanić, "Effect of the substrate material on diamond CVD coating properties," *Materials Chemistry and Physics*, vol. 80, pp. 529-536, 5/26/ 2003.

[20] G. W. Yang and B. X. Liu, "Kinetic model for diamond nucleation upon chemical vapor deposition," *Diamond and Related Materials*, vol. 9, pp. 156-161, Feb-Mar 2000.

[21] K. Subramanian, W. P. Kang, J. L. Davidson, and W. H. Hofmeister, "The effect of growth rate control on the morphology of nanocrystalline diamond," *Diamond and Related Materials*, vol. 14, pp. 404-410, Mar-Jul 2005.

[22] K. Okada, "Plasma-enhanced chemical vapor deposition of nanocrystalline diamond," *Science and Technology of Advanced Materials*, vol. 8, pp. 624-634, Oct-Nov 2007.

[23] F. A. Almeida, E. Salgueiredo, F. J. Oliveira, R. F. Silva, D. L. Baptista, S. B. Peripolli, *et al.*, "Interfaces in Nano-/Microcrystalline Multigrade CVD Diamond Coatings," *Acs Applied Materials & Interfaces*, vol. 5, pp. 11725-11729, Nov 2013.

[24] N. Govindaraju and R. N. Singh, "Processing of nanocrystalline diamond thin films for thermal management of wide-bandgap semiconductor power electronics," *Materials Science and Engineering B-Advanced Functional Solid-State Materials*, vol. 176, pp. 1058-1072, Aug 2011.

[25] T. F. Zeng and G. Chen, "Phonon heat conduction in thin films: Impacts of thermal boundary resistance and internal heat generation," *Journal of Heat Transfer-Transactions of the Asme*, vol. 123, pp. 340-347, Apr 2001.

[26] A. Majumdar, "MICROSCALE HEAT-CONDUCTION IN DIELECTRIC THIN-FILMS," *Journal of Heat Transfer-Transactions of the Asme*, vol. 115, pp. 7-16, Feb 1993.

[27] K. Jagannadham, "Model of interfacial thermal resistance of diamond composites," *Journal of Vacuum Science & Technology a-Vacuum Surfaces and Films*, vol. 17, pp. 373-379, Mar-Apr 1999.

[28] S. Bin Mansoor and B. S. Yilbas, "Phonon transport in silicon-silicon and silicon-diamond thin films: Consideration of thermal boundary resistance at interface," *Physica B-Condensed Matter*, vol. 406, pp. 2186-2195, May 2011.

[29] J. E. Graebner, S. Jin, G. W. Kammlott, J. A. Herb, and C. F. Gardinier, "UNUSUALLY HIGH THERMAL-CONDUCTIVITY IN DIAMOND FILMS," *Applied Physics Letters*, vol. 60, pp. 1576-1578, Mar 1992.

[30] Z. L. Wang, X. Tian, J. G. Liang, J. Zhu, D. W. Tang, and K. Xu, "Prediction and measurement of thermal transport across interfaces between semiconductor and adjacent layers," *International Journal of Thermal Sciences*, vol. 79, pp. 266-275, May 2014.

[31] D. T. Morelli, C. Uher, and C. J. Robinson, "TRANSMISSION OF PHONONS THROUGH GRAIN-BOUNDARIES IN DIAMOND FILMS," *Applied Physics Letters*, vol. 62, pp. 1085-1087, Mar 1993.

[32] C. P. Jen and C. C. Chieng, "Microscale thermal characterization for two adjacent dielectric thin films," *Journal of Thermophysics and Heat Transfer,* vol. 12, pp. 146-152, Apr-Jun 1998.
[33] G. Lucazeau, "Effect of pressure and temperature on Raman spectra of solids: anharmonicity," *Journal of Raman Spectroscopy,* vol. 34, pp. 478-496, Jul-Aug 2003.
[34] J. E. Graebner, M. E. Reiss, L. Seibles, T. M. Hartnett, R. P. Miller, and C. J. Robinson, "PHONON-SCATTERING IN CHEMICAL-VAPOR-DEPOSITED DIAMOND," *Physical Review B,* vol. 50, pp. 3702-3713, Aug 1994.
[35] K. E. Goodson, O. W. Kading, M. Rosler, and R. Zachai, "EXPERIMENTAL INVESTIGATION OF THERMAL CONDUCTION NORMAL TO DIAMOND-SILICON BOUNDARIES," *Journal of Applied Physics,* vol. 77, pp. 1385-1392, Feb 1995.
[36] K. E. Goodson, O. W. Kading, M. Rosner, and R. Zachai, "THERMAL CONDUCTION NORMAL TO DIAMOND-SILICON BOUNDARIES," *Applied Physics Letters,* vol. 66, pp. 3134-3136, Jun 1995.
[37] A. Gicquel, K. Hassouni, F. Silva, and J. Achard, "CVD diamond films: from growth to applications," *Current Applied Physics,* vol. 1, pp. 479-496, Dec 2001.
[38] J. E. Graebner and S. Jin, "Chemical vapor deposited diamond for thermal management," *Jom-Journal of the Minerals Metals & Materials Society,* vol. 50, pp. 52-55, Jun 1998.
[39] J. P. Mazellier, M. Mermoux, F. Andrieu, J. Widiez, J. Dechamp, S. Saada, *et al.*, "Enhanced thermal performances of silicon-on-diamond wafers incorporating ultrathin nanocrystalline diamond and silicon layers: Raman and micro-Raman analysis," *Journal of Applied Physics,* vol. 110, p. 9, Oct 2011.
[40] S. M. Lee and D. G. Cahill, "Heat transport in thin dielectric films," *Journal of Applied Physics,* vol. 81, pp. 2590-2595, Mar 1997.
[41] D. G. Cahill, "Heat transport in dielectric thin films and at solid-solid interfaces," *Microscale Thermophysical Engineering,* vol. 1, pp. 85-109, Apr-Jun 1997.
[42] J. E. Graebner, J. A. Mucha, L. Seibles, and G. W. Kammlott, "THE THERMAL-CONDUCTIVITY OF CHEMICAL-VAPOR-DEPOSITED DIAMOND FILMS ON SILICON," *Journal of Applied Physics,* vol. 71, pp. 3143-3146, Apr 1992.
[43] D. Das, R. N. Singh, S. Chattopadhyay, and K. H. Chen, "Thermal conductivity of diamond films deposited at low surface temperatures," *Journal of Materials Research,* vol. 21, pp. 2379-2388, Sep 2006.
[44] H. Relyea, M. White, J. J. McGrath, and J. V. Beck, "Thermal diffusivity measurements of free-standing CVD diamond films using non-contacting, non-destructive techniques," *Diamond and Related Materials,* vol. 7, pp. 1207-1212, Aug 1998.
[45] J. E. Graebner, H. Altmann, N. M. Balzaretti, R. Campbell, H. B. Chae, A. Degiovanni, *et al.*, "Report on a second round robin measurement of the thermal conductivity of CVD diamond," *Diamond and Related Materials,* vol. 7, pp. 1589-1604, Dec 1998.
[46] J. W. Monzyk, K. Lafdi, and K. W. Johnson, "Thermal diffusivity measurements of carbon materials using optical beam deflection," *Carbon,* vol. 38, pp. 1351-1359, 2000.
[47] O. W. Kading, E. Matthias, R. Zachai, H. J. Fusser, and P. Munzinger, "THERMAL DIFFUSIVITIES OF THIN DIAMOND FILMS ON SILICON," *Diamond and Related Materials,* vol. 2, pp. 1185-1190, May 1993.
[48] M. M. Gentleman, V. Lughi, J. A. Nychka, and D. R. Clarke, "Noncontact methods for measuring thermal barrier coating temperatures," *International Journal of Applied Ceramic Technology,* vol. 3, pp. 105-112, 2006.
[49] L. Fayette, B. Marcus, M. Mermoux, L. Abello, and G. Lucazeau, "Proceedings of the 4th European Conference on Diamond, Diamond-like and Related MaterialsIn-situ Raman investigation of diamond films during growth and etching processes," *Diamond and Related Materials,* vol. 3, pp. 438-442, 1994.

[50] M. Mermoux, L. Fayette, B. Marcus, N. Rosman, L. Abello, and G. Lucazeau, "IN-SITU RAMAN MONITORING OF THE GROWTH OF DIAMOND FILMS IN PLASMA-ASSISTED CVD REACTORS," *Diamond and Related Materials*, vol. 4, pp. 745-749, May 1995.
[51] E. Staryga, G. W. Bak, K. Fabisiak, L. Klimek, A. Rylski, A. Olborska, *et al.*, "Structure of diamond polycrystalline films deposited on silicon substrates," *Vacuum*, vol. 85, pp. 518-522, Oct 2010.
[52] V. Lughi and D. R. Clarke, "Temperature dependence of the yttria-stabilized zirconia Raman spectrum," *Journal of Applied Physics*, vol. 101, p. 6, Mar 2007.
[53] J. W. Ager, D. K. Veirs, and G. M. Rosenblatt, "SPATIALLY RESOLVED RAMAN STUDIES OF DIAMOND FILMS GROWN BY CHEMICAL VAPOR-DEPOSITION," *Physical Review B*, vol. 43, pp. 6491-6499, Mar 1991.
[54] J. B. Cui, K. Amtmann, J. Ristein, and L. Ley, "Noncontact temperature measurements of diamond by Raman scattering spectroscopy," *Journal of Applied Physics*, vol. 83, pp. 7929-7933, Jun 1998.
[55] P. V. Huong, R. Cavagnat, P. M. Ajayan, and O. Stephan, "TEMPERATURE-DEPENDENT VIBRATIONAL-SPECTRA OF CARBON NANOTUBES," *Physical Review B*, vol. 51, pp. 10048-10051, Apr 1995.
[56] M. R. Joya, A. R. Zanatta, and J. Barba-Ortega, "RAMAN SPECTROSCOPY OF TEMPERATURE INDUCED EFFECTS IN FOUR CARBON ALLOTROPES," *Modern Physics Letters B*, vol. 27, p. 10, Nov 2013.
[57] P. H. Tan, Y. M. Deng, Q. Zhao, and W. C. Cheng, "The intrinsic temperature effect of the Raman spectra of graphite," *Applied Physics Letters*, vol. 74, pp. 1818-1820, Mar 1999.
[58] M. Li and Y. A. Yue, "Raman-Based Steady-State Thermal Characterization of Multiwall Carbon Nanotube Bundle and Buckypaper," *Journal of Nanoscience and Nanotechnology*, vol. 15, pp. 3004-3010, Apr 2015.
[59] F. P. Incropera and D. P. De Witt, *Fundamentals of Heat and Mass Transfer*, 3rd ed.: John Wiley & Sons, Inc, 1990.
[60] N. Khosravian, M. K. Samani, G. C. Loh, G. C. K. Chen, D. Baillargeat, and B. K. Tay, "Molecular dynamic simulation of diamond/silicon interfacial thermal conductance," *Journal of Applied Physics*, vol. 113, p. 4, Jan 2013.
[61] M. S. Liu, L. A. Bursill, S. Prawer, and R. Beserman, "Temperature dependence of the first-order Raman phonon lime of diamond," *Physical Review B*, vol. 61, pp. 3391-3395, Feb 2000.
[62] N. V. Surovtsev and I. N. Kupriyanov, "Temperature Dependence of the Raman line width in diamond: revisited," *Journal of Raman Spectroscopy*, pp. 171-176, 2015.
[63] E. S. Zouboulis and M. Grimsditch, "RAMAN-SCATTERING IN DIAMOND UP TO 1900-K," *Physical Review B*, vol. 43, pp. 12490-12493, May 1991.
[64] I. Calizo, A. A. Balandin, W. Bao, F. Miao, and C. N. Lau, "Temperature dependence of the Raman spectra of graphene and graphene multilayers," *Nano Letters*, vol. 7, pp. 2645-2649, Sep 2007.
[65] R. J. Meier, "On art and science in curve-fitting vibrational spectra," *Vibrational Spectroscopy*, vol. 39, pp. 266-269, Oct 2005.
[66] G. Morell, O. Quinones, Y. Diaz, I. M. Vargas, B. R. Weiner, and R. S. Katiyar, "Measurement and analysis of diamond Raman bandwidths," *Diamond and Related Materials*, vol. 7, pp. 1029-1032, Jul 1998.
[67] R. Ramamurti, V. Sharlov, R. N. Singh, S. Mamedov, and P. Boolchand, "Raman spectroscopy study of the influence of processing conditions on the structure of polycrystalline diamond films," *Journal of Vacuum Science & Technology A*, vol. 24, pp. 179-189, Mar-Apr 2006.
[68] E. S. Etz, W. S. Hurst, and A. Feldman, "Correlation of the Raman spectra with the thermal conductivity of a set of diamond wafers prepared by chemical vapor deposition," *Journal of Materials Research*, vol. 16, pp. 1694-1711, Jun 2001.
[69] A. M. Zaitsev, *Optical Properties of Diamond*. Verlag Berlin Heidelberg: Springer, 2001.

[70] T. R. Hart, R. L. Aggarwal, and B. Lax, "TEMPERATURE DEPENDENCE OF RAMAN SCATTERING IN SILICON," *Physical Review B-Solid State,* vol. 1, pp. 638-&, 1970.
[71] R. Tsu and J. G. Hernandez, "TEMPERATURE-DEPENDENCE OF SILICON RAMAN LINES," *Applied Physics Letters,* vol. 41, pp. 1016-1018, 1982.

VITA

Marshall Addison Harrup

Candidate for the Degree of

Master of Science

Thesis: THERMAL CONDUCTIVITY OF DIAMOND THIN-FILMS ON SILICON WAFERS

Major Field: Materials Science and Engineering

Biographical:

Education:

Completed the requirements for the Master of Science in Materials Science and Engineering at Oklahoma State University, Stillwater, Oklahoma in December, 2015.

Completed the requirements for the Bachelor of Science in Engineering Physics at Oral Roberts University, Tulsa, Oklahoma in 2013.

Experience:

Graduate Research Assistant under Dr. Raj Singh from 2013-2015